THERMORESPONSIVE SMART POLYMERIC CELL CARRIERS OF
PNIPAM AND ELP FOR BONE TISSUE ENGINEERING

A THESIS SUBMITTED TO
THE GRADUATE SCHOOL OF NATURAL AND APPLIED SCIENCES
OF
MIDDLE EAST TECHNICAL UNIVERSITY

BY

NİHAN ÖZTÜRK

IN PARTIAL FULFILLMENT OF THE REQUIREMENTS
FOR
THE DEGREE OF MASTER OF SCIENCE
IN
BIOTECHNOLOGY

MAY 2008

Approval of the thesis:

**THERMORESPONSIVE SMART POLYMERIC CELL CARRIERS OF
PNIPAM AND ELP FOR BONE TISSUE ENGINEERING**

submitted by **NİHAN ÖZTÜRK** in partial fulfillment of the requirements for
the degree of **Master of Science in Biotechnology Department, Middle
East Technical University** by,

Prof. Dr. Canan Özgen   _____
Dean, Graduate School of **Natural and Applied Sciences**

Prof. Dr. Gülay Özcengiz   _____
Head of Department, **Dept. Biological Sciences**

Prof. Dr. Vasıf Hasırcı   _____
Supervisor, **Dept. Biological Sciences, METU**

Assoc. Prof. Dr. Gamze Torun Köse   _____
Co-Supervisor, **Dept. Genetics and Bioeng., YU**

Examining Committee Members:

Prof. Dr. Nazmi Özer   _____
Dept. Biochemistry, Fac. Medicine, Hacettepe Univ.

Prof. Dr. Vasıf Hasırcı   _____
Dept. Biological Sciences, METU

Prof. Dr. Meral Yücel   _____
Dept. Biological Sciences, METU

Prof. Dr. Faruk Bozoğlu   _____
Dept. Food Engineering, METU

Assoc. Prof. Dr. Ayşe Gül Gözen   _____
Dept. Biological Sciences, METU

Date: 12.05.2008

I hereby declare that all information in this document has been obtained and presented in accordance with academic rules and ethical conduct. I also declare that, as required by these rules and conduct, I have fully cited and referenced all material and results that are not original to this work.

Name, Last name : Nihan Öztürk

Signature   :

ABSTRACT

THERMORESPONSIVE SMART POLYMERIC CELL CARRIERS OF PNIPAM AND ELP FOR BONE TISSUE ENGINEERING

Öztürk, Nihan

M.S., Department of Biotechnology

Supervisor   : Prof. Dr. Vasıf Hasırcı

Co-Supervisor : Assoc. Prof. Dr. Gamze Torun Köse

May 2008, 77 pages

This study was aimed at designing a cell carrier from an intelligent polymer to achieve loading of mechanical stress for the purpose of improving the tissue engineering capability *in vitro*.

Ethyleneglycoldimethacrylate (EGDMA) crosslinked poly(N-isopropylacrylamide) (pNIPAM) films were prepared by radical polymerization with ultraviolet light (UV) in the presence of photoinitiator 2,2$^{\prime}$-azoisobutyronitrile (AIBN) in isopropanol/water (1:1). Patterns were formed on the surface of the polymers by using silicon wafers with microridges (2 µm) and grooves (10 µm) that were prepared by photolithography technique as the template. The surfaces of the films were also modified by adsorption of ELP-RGD6 polypeptide.

Bone marrow stem cells (BMSCs) isolated from 6 week old Sprague-Dawley rats were seeded onto the pNIPAM films with different surface topography and chemistry and cultured under static and dynamic conditions. Dynamic conditions were generated by cyclic temperature changes (15 min at 29°C, 30 min at 37°C) for 10 times a day during 5 days starting on the second day post-cell seeding.

ELP-RGD6 on the films enhanced initial cell attachment but had no effect on proliferation in long term culturing. However, for the dynamic culturing, ELP was crucial for both retaining cells attached on the surface when the surface became hydrophilic and resulted in weakened cell attachment, and for better communication between cell and material which enhanced the ability of pNIPAM films to transfer mechanical stress on the cells. Dynamic conditions improved cell proliferation but decreased differentiation. Presence of the patterns also influenced the differentiation but did not affected proliferation.

Keywords: Thermoresponsive, pNIPAM, Mechanical Stress, Bone Tissue Engineering

ÖZ

KEMİK DOKU MÜHENDİSLİĞİ İÇİN PNIPAM VE ELP TEMELLİ ISIYA DUYARLI AKILLI POLİMERİK HÜCRE TAŞIYICILARI

Öztürk, Nihan

Yüksek Lisans, Biyoteknoloji Bölümü

Tez Yöneticisi   : Prof. Dr. Vasıf Hasırcı

Ortak Tez Yöneticisi : Doç. Dr. Gamze Torun Köse

Mayıs 2008, 77 sayfa

Bu çalışmada amaçlanan, *in vitro* ortamda doku mühendisliği yetisini geliştirmek için, akıllı bir polimerden mekanik stres uygulayabilen bir hücre taşıyıcısının tasarlanmasıydı.

Etilenglikoldimetakrilat (EGDMA) ile çapraz bağlanan poli(N-izopropilakrilamid) (pNIPAM) filmler radikal polimerizasyonla fotobaşlatıcı $2,2^*$-azoisobutironitril varlığında ultraviyole ışıkla izopropanol/su (1:1) içinde hazırlanmıştır. Fotolitografi tekniğiyle hazırlanan mikro tepecik (2 µm) ve mikrokuyucuklu (10 µm) silikon pullarla polimerlerin yüzeyleri desenlendirilmiştir. Filmlerin yüzeyleri ayrıca ELP-RGD6 polipeptidinin adsorpsiyonuyla modifiye edilmiştir.

6 haftalık Sprague-Dawley sıçanlardan izole edilen kemik iliği kök hücreleri, farklı yüzey topografisi ve kimyası olan pNIPAM filmler üzerine ekilmiş ve statik ve dinamik koşullarda kültüre edilmiştir. Dinamik koşullar hücre ekiminden iki gün sonra başlatılarak 5 gün boyunca günde 10 kez periyodik sıcaklık değişimleriyle (15 dakika 29°C, 30 dakika 37°C) oluşturulmuştur.

Filmlerin yüzeyindeki ELP-RGD6, başlangıçtaki hücre tutunmasını arttırmış ama uzun dönem kültürde, bu proteinin çoğalma üzerinde etkisi olmamıştır.

Bununla birlikte dinamik kültürde yüzeyin hidrofilikliği arttığında ve bunun sonucu olarak hücre tutunması zayıfladığında, hücreleri yüzeye bağlı tutmak için ve pNIPAM filmlerin hücrelere mekanik stresi aktarma özelliğini arttıran daha iyi bir hücre-malzeme iletişimi kurulmasında önemli olmuştur. Dinamik kültür koşulları hücre çoğalmasını arttırmış, fakat diferensiyasyonu düşürmüştür. Yüzey desenlerinin varlığı diferensiyasyonda etkili olmuş, ama hücre çoğalmasını etkilememiştir.

Anahtar Kelimeler: Isıya Duyarlı, pNIPAM, Mekanik Stres, Kemik Doku Mühendisliği

Dedicated to My Family and to the Memories of
my Dear Grandpa "Faik İlter" and
my Dear Grandma "Kezban Öztürk"

ACKNOWLEDGEMENTS

I would like to thank firstly to my supervisor Prof. Dr. Vasıf Hasırcı, for his support, scientific guidance and help throughout this study.

I thank Assoc. Prof. Dr. Gamze Torun Köse for her contributions to this study as my co-supervisor.

I want to express my special thanks to my dear labmates Albana Ndreu, Banu Bayyurt, Hayriye Özçelik, Halime Kenar, Deniz Yücel, Beste Kınıkoğlu, Arda Büyüksungur, Aysel Kızıltay, Tuğba Endoğan, Pınar Yılgör, N. Engin Vrana, Erkin Aydın, Pınar Zorlutuna, Buket Başmanav, İ. Doğan Günbaş and Taylan Özerkan and our technician Zeynel Akın for their help and support during this study.

I am also grateful to my Aikido instructor Barış Şentuna and all the members of ODTU Aikido dojo for their friendship.

I want to express my special thanks to Prof. J. Carlos Rodríguez Cabello, Prof. Javier Arias, Dr. Alessandra Girotti, Dr. Ana María Testera, Susana Prieto, Artur Ribeiro, Javier Reguera, Jorge Gil and Alberto Sánchez for their hospitality, kindness, help and friendship during my visit to University of Valladolid, Spain.

I thank METU Central Laboratory for analyses done in their facilities.

I thank my dear family for their support, love, caring and the altruism they showed for my education throughout all these years we spent apart.

Finally, I want to express my most sincere gratitudes to "my sunshine" who has always been with me with love, support, understanding and caring and encouraged me in my most dispirited times.

TABLE OF CONTENTS

LIST OF TABLES

LIST OF FIGURES

LIST OF ABBREVIATIONS

AIBN   2,2ʳ-azoisobutyronitrile

ALP   Alkaline Phosphatase

APS   Ammonium Persulfate

BMA   N-Butyl methacrylate

BMP-2   Bone Morphogenetic Protein-2

BMSCs   Bone Marrow Stem Cells

CA   Carbonated Apatite

3D   Three Dimensional

DMEM   Dulbecco's Modified Eagle Medium

DMSO   Dimethylsulfoxide

Dy   Dynamic

ECs   Endothelial Cells

ECM   Extracellular Matrix

EGDMA   Ethylene glycol dimethacrylate

ELP   Elastin-Like Polypeptide

ELP-RGD   Elastin-Like Polypeptide Containing 'RGD' sequences

FCS   Fetal Calf Serum

hADAS   Human Adipose Derived Adult Stem Cells

HAp   Hydroxyapatite

HCs   Hepatocytes

ITT   Internal Transition Temperature

IPTG   Isopropyl-β-D-Thiogalactopyranoside

LB   Luria-Bertani Broth

LBA   Luria-Bertani Agar

LCST   Lower Critical Solution Temperature

NASI   N-Acryloxysuccinimide

NIPAM   N-Isopropylacrylamide

P   Patterned

PBS   Phosphate Buffered Saline

PCL   Poly(ε-caprolactone)

PGA	Poly(glycolic acid)
PHAs	Polyhydroxyalkanoates
PHB	Poly(3-hydroxybutyrate)
PHBV	Poly(3-hydroxybutyrate-co-3-hydroxyvalerate)
PLA	Poly(lactic acid)
PLGA	Poly(lactic acid-co-glycolic acid)
P(L,DL)LA	Poly(L,DL) Lactic Acid
PLLA	Poly L-Lactic Acid
pNIPAM	Poly(N-isopropylacrylamide)
PMSF	Phenylmethylsulphonyl
PPF	Poly(propylene fumarate)
RGD	Arginine-Glycine-Aspartic acid
SDS	Sodium Dodecyl Sulphate
SDS-PAGE	Sodium Dodecyl Sulphate Polyacrylamide Gel Electrophoresis
SEM	Scanning Electron Microscope
SMCs	Smooth Muscle Cells
St	Static
TB	Terrific Broth
TBS	Tris Buffered Saline
TCP	Tissue Culture Polystyrene
β-TCP	Beta Tricalcium Phosphate
TEMED	Tetramethylenediamine
Trypsin-EDTA	Trypsin-Ethylenediamine Tetra-Acetic Acid
UP	Unpatterned
UV	Ultraviolet
XPS	X-Ray Photoelectron Spectroscopy

CHAPTER 1

INTRODUCTION

1.1 Tissue Engineering

Due to aging, diseases or injury, many people suffer from malfunctioning of tissues, which may even lead to organ failure. Organ transplantation, prosthesis and tissue grafting are the treatments used in medicine to meet these problems. Although they have revolutionized medical practice, they still have limitations. For organ transplantation, it is mostly hard to find a genetically identical organ and in most of the cases the organ transplanted is from another person that is not genetically identical but with high conformity, which is called an allograft. However the insufficiency of donors leads to the death of many people due to the long period they may wait in order to find a suitable organ. Patients who survive after a successful transplantation still need to use costly immunosuppressive drugs that lower their quality of life. Autologous tissue grafting is also limited by the availability of host tissue and donor site morbidity. Prosthesis cause problems like material failure that lead to immunogenic response and increased rates of infection and since it is nonliving, it can not grow with the patient or adapt to changing circumstances [1].

Tissue engineering has emerged as a promising research area with a high potential to replace these conventional medical treatments by producing biological substitutes to restore, maintain or enhance tissue and organ function by combining biological understanding and applications with engineering principles. The early studies started from 1970s and progressed enormously in the last decade of 20th century reaching to clinically available medical therapeutics, yet need to be improved [2].

1

We can classify tissue engineering applications broadly into two categories: therapeutic applications, where the tissue is either grown in a patient or grown outside the patient and transplanted; and diagnostic applications, where the tissue is formed *in vitro* and used for testing drug metabolism and uptake, toxicity, pathogenecity, and so on [2].

The complexity and highly organized structure of human body makes it a big challenge for researchers to achieve the goal of engineering a desired tissue. Various disciplines need to be involved to analyze tissue dynamics and recreate it such as cell biology, biochemistry, biomechanics, biophysics and materials science. To generate a living tissue *in vitro* we need 1) cells, which will form the desired tissue or tissue groups, 2) scaffold or a cell carrier that host cells help them to grow and get organized in the way they are in the body and 3) surrounding media composed of nutrients, essential amino acids, and biological stimulants such as differentiation and growth factors.

1.2 Bone Tissue Engineering

The loss of bone because of trauma, cancer, osteoporosis or congenital abnormalities is a big clinical problem. High costs theraphies still do not provide a qualified life because many problems arise afterwards. The most common methods to repair these defects are through autologous grafting or using alloplastic implants which are nonbiological materials [3,4]. Autologous tissue grafting is the prevalent and most versatile option in most cases but has constraints such as the availability of donor tissue, morbidity at the donor site, and time-consuming surgery. Alloplastic implants are readily available and do not lead to donor site morbidity, but there is a risk of immune rejection and transfer of infectious diseases during the surgery. Moreover they are not long-lasting and biomaterial failure and incompatibility due to wear or corrosion may cause complications like chronic irritation and sometimes even carcinogenicity [4].

As an alternative approach, tissue engineering seems promising as it aims to create fully functional and biocompatible "living" grafts in sufficient amounts that have the potential to integrate with the surrounding native tissue

2

eliminating problems of donor scarcity, supply limitation, pathogen transfer and immune rejection [5, 6].

1.3 Scaffolds

A tissue engineered product is composed of two main components, the cells and their carrier. Named 'scaffold', its design is a crucial step in tissue engineering process since the rate of success of tissue engineering depends significantly on this carrier. Its main function is that in combination with the cells of interest it should mimic the structure and function of the natural extracellular matrix (ECM). Polymeric scaffolds, especially biodegradable ones, have attracted the attention of the researchers in the last decades. There exists a variety of scaffold preparation methods, among which are solvent casting, gas foaming, phase separation, electrospinning, salt leaching and self-assembly [7,8]. These scaffolds may be prepared in different forms such as films [9,10], foams [11] or fibers [7].

Due to its importance in tissue engineering and regenerative medicine there are some certain minimum requirements that the scaffold should possess. First of all, it needs to have an appropriate microstructure and chemical composition so that the cells can communicate well with it. Porosity is an important parameter that should be taken into consideration while designing a tissue engineering scaffold (even though the exact specifications depend on the type of tissue that will be produced). The pore diameter, size, distribution and orientation are chosen depending on the target tissue. A pore size of hundred microns has been reported for housing of osteoblasts and blood vessels. Microporosity (pore size below 10 μm) is also crucial since it is important for protein adhesion, cell attachment and proliferation, and for nutrient and waste product exchange [12-14]. Many studies have shown that pore size, shape and density of scaffolds have a significant effect on the behavior of cells [14,15].

The chemical structure of the materials used is known to have an influence on cell behavior to a great extent. In cases when the properties of the bulk material is suitable for tissue engineering but the chemistry is not, surface

treatments like exposure to UV [16], plasma treatment [7], grafting of chemical and biological entities [17] are applied to modify the surface properties of scaffolds.

Two other important requirements of the scaffold are that it should be biocompatible and biodegradable. The degradation properties (mainly the rate) of the material are again chosen by taking the target tissue into consideration. It is important to consider the products of degradation; mainly no toxic materials should be released into the biological medium. The degradation rate of the scaffold material can be altered by changing its chemistry, adding other components such as ceramics [18,19] or by altering the manufacturing methods [19-21]. Finally, the newly formed tissue should be able to withstand the load that may be created on it when *in vivo,* therefore, the mechanical properties of the scaffold material that is employed are of great importance [22,23]. It has been found that the efficacy of several silk- and collagen-based substrates in supporting chrondrogenesis of cultured human mesenchymal stem cells was influenced more by scaffold degradation rates than by chemical composition [24]. Crosslinked collagen and slowly degrading silks increased cell differentiation and matrix deposition, but the uncrosslinked collagen samples were unable to support significant cartilaginous tissue formation because of weak mechanical property.

There are many crucial roles that a tissue engineered scaffold plays; it acts as a framework and supports cell migration from the surrounding tissue into the defect area, it serves as a matrix for endogenous or exogenous cell adhesion and facilitates cell processes like proliferation, migration and synthesis, it may be used as delivery vehicle of certain genes for certain growth factors or growth factors themselves, it may structurally reinforce the defect area, it may also serve as a barrier against infiltration of the surrounding tissue that may hinder the regeneration process [22].

1.3.1 Materials

The materials utilized in the design of tissue engineering scaffolds can be classified as metals and metal alloys, ceramics, polymers, modified natural materials and composites. Based on their degree of resorbability they can be

divided into two groups: degradable and non-degradable. Non-degradable materials are usually used for prosthetic devices whereas resorbable ones are mainly used for tissue regeneration like bone, cartilage, artificial skin, etc. [25]. Degradability has been shown to be important since the surface properties of the material used influence to a great extent the initial cellular events occuring at the contact phase between the cell and the material.

Regarding their application as scaffold materials in tissue engineering or as bone substitute materials it can be said that four types of materials have been studied. They include the synthetic organic materials (polyglycolides, polylactides, polydioxanone, polycaprolactone, polyanhydrides, polyhydroxyalkanoates, etc.), synthetic inorganic materials (hydroxyapatite, glass ceramics, etc.), organic materials of natural origin (collagen, hyaluronic acid, elastin, fibrin, etc.) and inorganic materials of natural origin (coralline HA) [25]. The following section explains these materials in more detail.

1.3.1.1 Degradable polymers

Bioabsorbable polymers are preferred because they can be employed to provide temporary scaffolding function for newly forming tissue and to be subsequently replaced by the native tissue with the polymer material getting removed by natural and metabolic processes of the body. Hence, no residual material that can act as focus of irritation with possible infection is left in the body. It is also important for the newly formed tissues to take over by time and become independent of the supporting scaffold. This is especially important, e.g. in tissues like bone where physiological loading is crucial.

The main polymers utilized with the ultimate aim of tissue engineering include poly L-lactic acid (PLLA), poly (L,DL) lactic acid P(L,DL)LA, poly(ϵ-caprolactone) (PCL) or their copolymers like poly(lactic acid-co-glycolic acid) (PLGA) and poly(ϵ-caprolactone-*co*-L-lactide) (PCL-PLLA) etc. Polymers of natural origin include collagen, silk protein, elastin, fibrinogen, fibrin, chitosan, hyaluronic acid and poly(3-hydroxybutyrate-co-3-hydroxyvalerate) (PHBV) [26,27]. These types of natural polymers are often used in the form of blends with some other materials like ceramics (especially in bone tissue

engineering) in order to increase their load bearing ability, thus, strengthen their mechanical properties [28-30].

Collagen is a natural fibrous protein found most abundantly in the extracellular matrix of the body, in tissues like bone, tendon, cartilage, ligament, skin, meniscus, etc. Due to the differences in chemical composition and molecular structure collagen has 25 different types, the most abundant ones being types I, II, III and V. While type I is more present in bone and meniscus, type II is more found in cartilage. It is widely used in tissue engineering applications; however, crosslinking is sometimes necessary in order to improve the mechanical properties of the collageneous scaffold [24,27,28,31].

Elastin is a protein found in connective tissue to help to resume the shape after stretching or contracting. It is most abundantly found in load-bearing tissues such as arteries, lungs, elastic ligaments, skin, bladder, elastic cartilage, and the intervertebral disc. It is primarily composed of the amino acids glycine (G), valine (V), alanine (A) and proline (P).

Genetically engineered artificial elastin-like polypeptides (ELPs) possess physical properties that are notably similar to those of native elastin. The crosslinked matrices of ELPs show outstanding resistance to fatigue and have almost ideal elasticity, with Young's modulus, elongation at break, etc. in the range of natural elastin [32,33]. Moreover, these proteins can be modified at the genetic level to match the requirements of desired applications, such as addition of cell attachment sequences and amino acids to use for crosslinking purposes i.e. lysine [34]. The general formula for ELPs is $(VPGXG)_n$, where X represents any natural or modified amino acid, except proline [35].

Fibrin is a polypeptide and has an important role in tissue repair and homeostasis. This substance is produced by polymerization of fibrinogen in the presence of enzyme thrombin and as a result clotting occurs. It can either be obtained directly from blood plasma of patients [36]. It is not a part of ECM but it has been used especially for wound closure as a matrix that can be

replaced by the ECM. It is widely used as fibrin glue in clinical applications. Its combination with alginate or hyaluronic acid has been demonstrated [31].

Hyaluronic acid, known as hyaluronan, is a linear, high molecular weight polysaccharide and it is one of those glucosaminoglycans present in the connective tissues of the body, in the eye vitreus humor and the synovial fluid of the joint capsule. Due to its disaccharide units, hyaluronic acid has a rigid structure and its anionic groups function in binding water molecules and other cations. They appear to be very good water absorbers and lubricants due to its viscoelastic properties. They play a crucial role in wound repair, morphogenesis and inflammation [31,37,38,39].

Chitosan is a deacetylated chitin derivative mostly found in the shells of marine crustaceans and the walls of fungal cells. It is soluble in dilute acids. This linear polysaccharide is attractive for researchers because it is biodegradable, highly biocompatible, it has controllable hydrophilicity (with deacetylation level) and it is easy to process. Chitin-based polymers can be processes into various forms like sponges, fibers, hydrogels and beads, and this is a good proof of its versatility of its biomedical applications especially tissue engineering. Other physicochemical and biological properties of chitosan in addition to hydrophilicity can be altered by changing the deacetylation degree [31,40].

Another class of naturally derived polymers is polyhydroxyalkanoates (PHAs), which are polyesters produced by microorganisms [41]. They are degradable and biocompatible and are used as a reserve of energy and carbon. A variety of these polymer were produced and among especially poly(3-hydroxybutyrate) (PHB) and its copolymer poly(hydroxybutyrate-co-hydroxyvalerate) (PHBV) have been tested the most in the biomedical field. Addition of hydroxyvalerate to the structure results in a less crystalline, more flexible and easily processable polymer, so depending on the amount of degradability and crystallinity desired, an appropriate copolymer is synthesized [31]. Among the PHAs, PHB is of particular interest due to its ability to support *in vitro* bone formation [42,43].

Recently, proteins obtained from animals or plants have started to attract the researcher's attention significantly nowadays. A good example of these proteins is silk, which is produced in fiber form by silkworms and spiders. The high mechanical properties of silk come as a result of the highly repetitive primary sequence that leads to a high content of β-sheets [31]. This is a good reason that explains potential of silk protein in tissue engineering processes, especially in the case when mechanically robust and sufficiently degradable materials are required [44]. The only disadvantage of utilizing this material is that it might evoke foreign body responses when implanted *in vivo* [31].

Like the natural polymers, synthetic polymers are also in a great variety and due to the results obtained many of them have been approved by FDA to be used in tissue engineering applications. Compared to natural polymers, they have shown lower risk of immunogenicity, easier procesability and higher flexibility. As mentioned in the sections above, the most common synthetic polymers are, poly(ε-caprolactone) (PCL), poly(glycolic acid) (PGA), poly(lactic acid) (PLA), their copolymers poly(lactic acid-co-glycolic acid) (PLGA), poly(phosphoesters), poly(phosphazene), and poly(propylene fumarate) (PPF). Some of them will be described in more detail below:

PLA, PGA and PLGA (with different ratios of LA and GA) are the most intensively investigated synthetic polymers in tissue engineering, especially bone. Upon reaction with water they undergo random bulk degradation via hydrolysis of ester bonds which results in their degradation products namely lactic and glycolic acids [45]. PLA exists in mainly three forms: L-PLA (PLLA), D-PLA (PDLA) and the racemic mixture D,L-PLA (PDLLA) with the main difference between them being stereochemistry. PLA is known to be less degradable and more hydrophilic than PGA [45]. The most utilized polymer in tissue engineering is PLGA, which is chosen according to the ratio of LA and GA in its structure because this detemines their crystallinity, hydrophilicity and their rate of degradation. For instance, if a highly degradable polymer is required, a blend with a LA:GA ratio of around 1 is preferred [46].

Another important synthetic polyester is poly(ε-caprolactone) (PCL), which is also a linear polymer with a slower degradation rate than most biodegradable polymers [47,48].

1.3.1.2 Non-degradable materials

The most commonly used non-degradable materials for tissue engineering, especially bone, are ceramics and its composites with polymers. Ceramics are mostly considered as crystalline materials, but there exist some non-crystalline ceramics also. When the glass is semi crystalline due to later heat treatments, it is known as glass-ceramic. A combination of both these two types and some others constitute what is named as composites. Composites have been utilized more in the last decade due to their versatility, the presence of many different composites with different structures suitable for various applications. Some composites are listed below:

A. Calcium phosphate-based ceramics. These include (1) hydroxyapatite (HAp), (2) beta-tricalcium phosphate (β-TCP), (3) biphasic calcium phosphate (BCP), (4) amorphous calcium phosphate (ACP), (5) carbonated apatite (CA) and (6) calcium deficient HAp (CDHAp). Their application in tissue engineering is still being explored, however, it can be said that the problem of incomplete resorption especially in the case of HAp or CA still exists. Introduction of porosity to the structure is an important issue that should be taken into consideration since it is well known that highly porous implants induce tissue ingrowth within the implant and decrease degradation time. This can be achieved by a variety of methods that lead to structures with interconnected pores [29]. Salt leaching and incorporation of polymeric microparticles that can be sintered afterwards to yield ceramics with micropores are two of these techniques. Furthermore, some surfactant (i.e. H_2O_2) can be utilized to produce spherical porosity inside the CaP-ceramic. In addition to these, some of the ceramics like bovine derived ones might possess inherent porosity but they are disadvantageous in that they cannot be tailored for specific purposes due to their fixed shape and volume. Some other CaP-ceramics have micro/nanoporosity, which is not very preferred in tissue engineering applications because of the pore size being close or lower than that of the

cells. The most appropriate tissue engineering application for them is bone tissue engineering since these CaP-based ceramics had a positive influence on cell differentiation and proliferation. Addition of osteoinductive growth factors or drugs [49] to these ceramics is also a common method due to their high affinity for ionic molecules. Utilization of ceramics with self-osteoinductive properties, such as biphasic calcium phosphate and HAp [50] is another way to improve their suitability for tissue engineering.

B. Calcium phosphate-based cements (a powder phase of calcium and/or phosphate salts that together with an aqueous phase react at room/body temperature and form a calcium phosphate precipitate that sets in the form of crystals). Cements based on calcium salts, phosphates or sulphates, have attracted much attention in medicine and dentistry due to their excellent biocompatibility and bone-repair properties. Many of them are attractive for use in tissue engineering, but the introduction of a crucial characteristic like porosity is a necessity. Highly porous systems can be obtained by either utilizing leaching of water soluble crystals [51] or degradation of polymer microspheres with time [29]. The polymer is chosen according to its degradation properties. The porosity of the structure and the mechanical properties depend on the cement formulation and whether there is any additive or not [52,53].

Calcium phosphate cements which can be injected and resorbed are prepared with slight differences in their compositions and/or processing. These cements are very compatible with the bone and seem to resorb slowly. During this gradually occurring resorption process the newly formed bone grows and replaces the cement. However, the properties of the calcium phosphate cements are still insufficient for their reliable application. There are problems related to their mechanical strength, the curing time, the application technique on the osseous defect and the final biological properties [53]. In addition, all the implants obtained from these materials can lead to infections due to their action as foreign materials for the body. In these situations some drugs, which can be locally released "in situ" are incorporated into the structure [54,55]. New improvements in the development of these cements

10

are being made in order to at least overcome some of these disadvantages [53].

C. Glass ceramics. They are reported to be bioactive due to their ability to bind to bone. This process happens due to formation of a CaP-rich layer which then crystallizes to carbonated hydroxyapatite on the surface of the glass after implantation and contact with biological fluids [56]. Several studies have shown that bioactive glasses support *in vitro* osteobast attachment, proliferation and differentiation of mesenchymal cells into osteoblasts [56-58].

These ceramics include glass compositions that have the ability to bind to bone and other tissues. The chemical reactivity of the glass where Si bonds are broken and the formation of a CaP-rich layer on the top of the glass, which then crystallizes to HCA is the basic idea of how bone binding process occurs. They are produced like conventional glasses where SiO_2, Na_2O, CaO and P_2O_5 are the basic components. These materials often need addition of other ceramic components for reinforcement due to their non-optimal mechanical properties. These types of combinations are named as glass-ceramic composites. Porosity is again a necessity for their ultimate use in tissue engineering applications and it is generally introduced as in the case of CaP-based ceramics [59].

D. Polymer/ceramic composites. Although ceramics seem to be excellent materials for use as scaffolds, they possess certain drawbacks. Brittleness and slow or no degradation and resorption are the main issues. In order to overcome these drawbacks ceramics are generally manufactured as composites, mostly of polymer-ceramic type. Addition of biodegradable polymers in the structure aims to improve the degradability, alter the mechanical properties of ceramics and create a porous structure. These composites also mimic the natural bone tissue composition of collagen and calcium phosphate. Several studies have reported the success of such designs in bone tissue engineering with better mechanical, osteoconductive (enable bone ingrowth) and osteoinductive (stimulate bone formation) properties [56].

11

As mentioned in the sections above, introduction of porosity to these ceramics materials is a necessity for especially tissue engineering applications. This has been solved by addition of some other molecules that can be destroyed before implantation, however, there still exits some problems such as poor degradability and mechanical properties. Mixing them with some biodegradable polymers is a solution to this at least to the majority of the problems. These biodegradable polymers can improve the degradability of these ceramics and further improve their mechanical properties [60]. Polymer/ceramic composites can be divided into two groups as cement with added polymers, and ceramic particles incorporated into a porous polymeric carrier. Some of the polymers combined with ceramics are polylactic/polyglycolic acid, polylactid acid (PLA, PLLA, PDLLA), polyglycolic acid (PGA), poly(lactic-co-glycolic acid) (PLGA), poly(ε-caprolactone) (PCL), collagen, gelatin, fibrin, casein, peptides, chitin, chitosan, cellulose, starch, alginate, hyaluronan, etc.

1.3.1.3 Stimuli-Responsive Polymers

Stimuli-responsive polymers are defined as polymers that exhibit dramatic property changes in response to small external changes in the environmental conditions.

They can be classified according to the stimuli they respond to. The stimulus can be physical such as temperature, electric or magnetic fields, and light, which alter molecular interactions. Chemical stimuli, such as pH, ionic strength and chemical agents, change the interactions of polymer chains among each other or between polymer chains and solvents at the molecular level [61]. Some polymers can respond to more than one stimulus, such as temperature and pH [62-65], and some polymers can also respond to two or more signals when they are simultaneously applied such as in dual responsive polymer systems which can find application in drug delivery [66].

These polymers can be utilised in various physical forms such as free chains in solutions, chains grafted on a surface, covalently cross-linked gels and reversible (or physical) gels [67].

Smart systems can be designed for biomedical applications using stimuli responsive polymers such as intelligent on-off systems for bioseperation [68-70], actuation [71-73], gene [74,75] and drug delivery [66,76-81], tissue engineering and cell culture [82-104].

Cell sheet engineering has emerged as one of the outcomes of this intense research area. Okano et al. published a paper in 1990 which made a great impact on the biomaterials and tissue engineering community [90]. The paper was describing the development of a novel cell culture substrate to harvest and expand cells. The researchers grafted the surface of tissue culture plates with a thermoresponsive polymer, poly(N-isopropylacrylamide) (pNIPAM), which has a lower critical solution temperature (LCST) around 32°C meaning that the polymer solution undergoes phase transition from a soluble to an insoluble state above this critical temperature in water [61]. This interesting property of LCST polymers is observed as a result of reversible hydrogen bond formation between water molecules and polar groups of the polymer such as C=O and -NH upon change in temperature leading the polymer to be hydrophilic below 32°C and hydrohopic above it (*Fig.* 1).

(a)

(b)
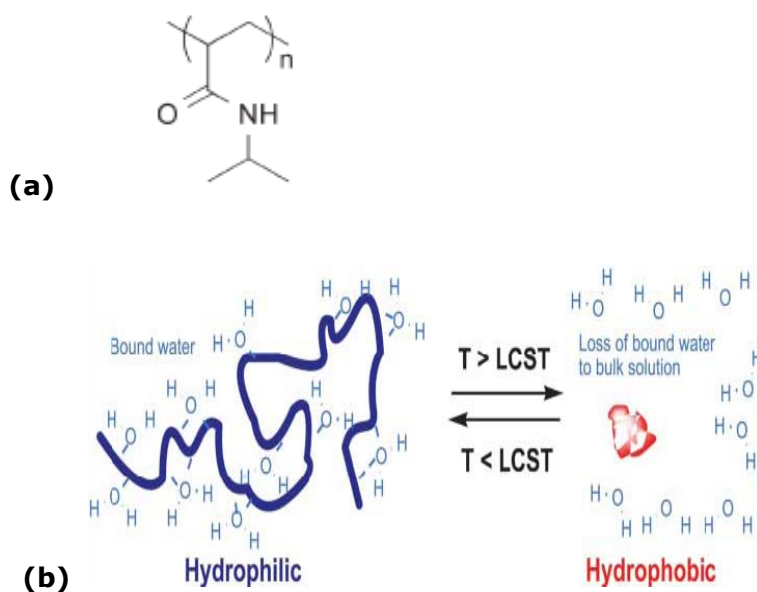
Figure 1. Poly(N-isopropylacrylamide), (a) Structure, (b) Schematic of 'smart' polymer response to temperature changes [91].

At normal cell culture temperature, which is 37°C, the polymer becomes slightly hydrophobic allowing various cell types to attach, spread and proliferate similarly to that on normal tissue culture polystyrene (TCP). However, when the temperature is reduced below the LCST, a hydration layer forms between the culture surface and cells and this weakens the attachment of cells, enabling the harvest of confluently cultured cells as intact sheets [92]. These cell monolayers with undistrupted intercellular connections, unlike those cells harvested by trypsinization are promising tools for successful tissue engineering applications. Numerous cell types including epidermal keratinocytes, vascular endothelial cells, renal epithelial cells, periodontal ligaments and cardiomyocytes have been shown to maintain differentiated functions after low-temperature cell sheet allowing production of vascularized thick tissues [93], cardiac patches [94], organ-like structures such as myocardial tubes [95] and reconstruction of cornea [96], esophagus [97] and trachea [98].

Single Layer Tissue

・ Skin

・ Corneal Epithelium

・ Periodontal Ligaments
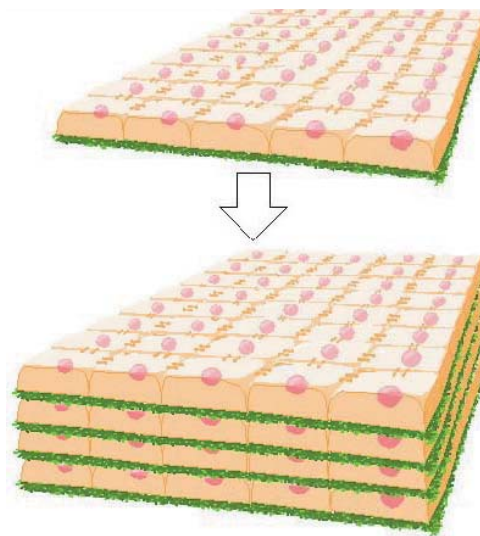
Multiple, Stratified Tissues

・ Myocardium

Figure 2. Schematic drawings of tissue reconstruction as cell sheet stacks using thermoresponsive culture dishes [99].

Furthermore, cell sheets composed of co-culture of different kinds of cells can also be harvested from patterned dual thermoresponsive surfaces with two kinds of thermoresponsive domains with different transition temperatures by copolymerization of a hydrophobic monomer to pNIPAM. In a study carried out by Tsuda et al., rat primary hepatocytes (HCs) and bovine carotid artery endothelial cells (ECs) were co-cultured on patterned dual thermoresponsive surfaces [100]. N-butyl methacrylate (BMA) was copolymerized with NIPAM to decrease the LCST. Patterns were prepared by electron beam copolymerization of these monomers using a mask led to islands of 1000 or 500 µm dots separated from each other by 1000 or 500 µm pNIPAM-grafted domains. First HCs were seeded at 27°C and they selectively adhered onto the relatively hydrophobic p(NIPAM–BMA) co-grafted domains but not onto the hydrophilic pNIPAM domains. They were incubated at 27°C for two days and at 37°C for an additional 2 days. Then the other cell type, the ECs, was seeded at 37°C. Finally, single co-cultured cell sheet could be released and recovered at a lower temperature than either of the transition temperatures (20°C) (*Fig.* 3). They showed that hepatic physiological functions such as albumin secretion and ammonium metabolism were enhanced by increasing heterotypic cell–cell interactions in a patterned co-culture. These findings indicate the importance of co-cultures for the reconstruction of complex tissues.
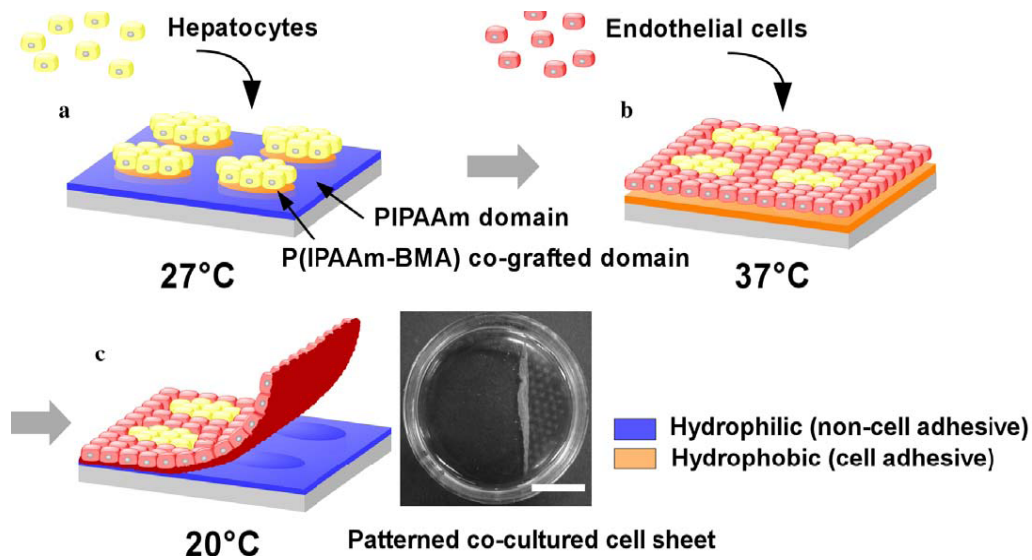
Figure 3. Schematic representation of patterning cell co-culture and harvesting of co-cultured cell sheets using a patterned dual thermoresponsive surface (a) First cell type, HCs is seeded and cultured at 27°C, resulting in localization of hepatocytes onto p(NIPAM–BMA) co-grafted hydrophobic patches. (b) Second cell type, ECs seeded and cultured at 37°C, resulting in generation of patterned co-cultures. (c) Decreasing temperature to 20°C enables obtaining the co-cultured cell sheet (on the right) [100].

Cell sheets harvested from thermoresponsive culture surfaces can be used for the reconstruction of many tissue types but may not be ideally suited to the creation of some cell-sparse tissues, such as bone or cartilage, because they contain relatively little ECM when compared with scaffold based methods [92].

Researchers are utilizing stimuli-responsive hydrogels as scaffolds in the engineering of tissues. Hydrogels can be applied as space filling agents, as delivery vehicles for bioactive molecules, and as three dimensional (3D) structures that organize cells and present stimuli to guide the formation of the desired tissue [101].

Stile and Healy prepared loosely crosslinked hydrogels composed of pNIPAM and acrylic acid (Aac) functionalized with RGD peptides as injectable scaffolds for cell attachment to study cell-material interactions in 3D [102]. They were the first to report covalent grafting of a large RGD peptide into NIPAM/Aac

hydrogels. These injectable hydrogels demonstrated increase in Young's modulus (i.e. rigidity) at the body temperature (37°C). Furthermore these injectable hydrogels were also synthesized by using peptide crosslinkers which can be splitted by matrix metalloproteinases, endopeptidases responsible for cleavage of extracellular matrix (ECM) proteins, adding a second property to the material which is biodegradability [103]. Increased adhesion and spreading of rat calvarial osteoblasts (RCO) to the hydrogel in the presence of the RGD peptide was shown.

Smith et al. prepared p(NIPAM/NASI), NIPAM-based synthetic, thermoresponsive copolymers containing protein-reactive N-acryloxysuccinimide (NASI) groups to increase local retention of bone morphogenetic protein-2 (BMP-2), which is one of the BMPs used for bone regeneration [17]. They utilized the thermoresponsiveness of pNIPAM to entrap and retain BMP-2 at the injection site (as much as 100 fold better), as the polymer solution became insoluble upon reaching the physiological temperature. They used C2C12 cells in their study and found out that the cells showed increased alkaline phosphatase (ALP) activity, which is one of the early markers showing the osteogenic differentiation, when they were on p(NIPAM-NASI) surfaces with BMP-2 rather than on tissue culture polystyrene (TCP) with BMP-2. Furthermore they showed that unlike cells on TCP, cells grown on the p(NIPAM/NASI) surfaces exhibited an ALP activity even without BMP-2 exposure, indicating that p(NIPAM/NASI) surfaces were more conductive for the expression of ALP activity for the chosen cell model.

Genetically engineered ELPs, mentioned in section 1.3.1.1, also are thermoresponsive polymers associated with the inverse transition temperature (ITT), a phenomenology which is similar to LCST. However, ELPs undergo a regular, non-random structure when the temperature is above the transition temperature, which is not shown by LCST polymers such as pNIPAM [31]. Phase transition behavior of an ELP is a function of the sequence, the identity and mole fraction of guest residues (X) at the fourth position of the general formula which is $(VPGXG)_n$, and its chain length [104].

The biosynthesis of the genetically engineered protein based polymers is superior over chemical synthesis in means of achieving absolute control of the amino acid sequence with complete absence of randomness. Moreover they can be easily produced in huge amounts using micro-organisms as factories to express these proteins [31]. Modification of sequence, chain length, topology and stereochemistry enables the controlling of physical properties such as transition temperature, mechanical stiffness and they can be functionalized to exhibit responsiveness to pH, light and other stimuli, such as an electrochemical potential or analyte concentration [77,105]. They are widely used in many fields of biotechnology including bioseparation [69,70], drug delivery [76,81] and tissue engineering [33,105].

They have been utilized to serve as injectable scaffolds for cartilaginous tissue repair because of their potential to promote chondrogenesis [105,106]. After injection *in situ,* similarly to pNIPAM, the ELP-chondrocyte suspension aggregates into a stiff gel-like coacervate when the temperature reaches the physiologic value entrapping cells within an elastic 3D matrix that has mechanical properties comparable to those reported for collagen and hyaluronan-based scaffolds which are commonly used for cartilage regeneration. Betre et al. examined the potential of a genetically engineered ELP to promote the chondrocytic differentiation of human adipose derived adult stem cells (hADAS) without exogenous chondrogenic supplements [105]. They observed that constructs cultured in either chondrogenic or standard medium (without chondrogenic supplements) exhibited significant increases in sulfated glycosaminoglycan and collagen contents by day 14. They also showed that the matrix formed consisted mainly of type II and not type I collagen and the composition of the constructs cultured in either medium did not differ significantly.

In order to manipulate the physical properties, ELPs may also be crosslinked enzymatically. McHale et al. designed and synthesized ELPs capable of undergoing enzyme initiated gelation via tissue transglutaminase [106]. The formed cartilaginous matrix was rich in type II collagen and lacking in type I collagen. They found out that the dynamic shear moduli of ELP hydrogels seeded with chondrocytes increased from 0.28 to 1.7 kPa during a 4 week

culture period indicating the restructuring of the ELP matrix by deposition of functional cartilage ECM components.

1.4 Mechanical Stimuli as a Modulator

Most of the cells in the body including fibroblasts, osteoblasts, chondrocytes, endothelial cells, and smooth muscle cells (SMCs) recieve mechanical stimuli from a wide variety of sources in daily life. These mechanical forces are gravity, compressive loads on cartilage and bones during walking and exercise; blood pressure and shear stresses on the vessels, the heart and the lung due to blood flow; tensile, compressive, and shearing forces causing surface tension on dermal tissues [107]. Tissues sense these mechanical stimuli and convert them into biological responses through a cascade of signal transduction resulting in regulation of cell functions like gene expression, cytoskeleton organization, protein synthesis, proliferation, apoptosis, and differentiation.

When the skeleton is unloaded due to microgravity in space flights and bed-rest, bone mineral density reduces [108]. On the other hand, suitable exercise regimes have been proposed to maintain bone mass in postmenopausal women and accelerate bone mass recovery after bed rest [109,110]. Mechanical loading is also important in fracture healing. These show that bone is a living organ that is modulated by mechanical stimuli. Bone tissues grow in a highly dynamic environment, experiencing both of compressive loads and tensile stress as well as fluid shear stress as a result of enhanced fluid flow in the canalicular network caused by mechanical loading [111].

In order to study the effect of mechanical stimuli on bone cells, several different devices have been used. These devices were usually designed to apply fluid flow [112,113], stretching and fluid flow using four point bending [114], hydrodynamic pressure [115], stretching and compression [116-120]. However, the reported answers vary widely and it is difficult to compare these results because of the variation in the devices and cell sources used. Moreover, parameters differ on the magnitude of the mechanical stress

applied as well as cycle number and the frequency of the strain in the studies [121].

1.5 Summary of the Used System

The aim of this study was to design a cell carrier with a capacity of loading mechanical stress on cells seeded onto them as an alternative to the devices mentioned in section 1.4. To achieve this goal, crosslinked pNIPAM films were used as cell carriers which have the ability to alter their dimensions in response to temperature changes below and above its LCST, ca. 32°C.

CHAPTER 2

MATERIALS AND METHODS

2.1 Materials

Poly(N-isopropylacrylamide) (pNIPAM), Coomassie Brillant Blue, Bromophenol Blue, APS, tetramethylenediamine (TEMED), buthanol, phenylmethylsulphonyl fluoride (PMSF), cacodylic acid (sodium salt), glutaraldehyde (Grade I, 25 % aqueous solution), Amphothericin B, Penicilline-Streptomycine, trypsin-EDTA (0.25 %), Trizma® Base, dimethyl sulfoxide (DMSO), B-glycerophosphate, ascorbic acid and dexamethasone were purchased from Sigma-Aldrich Co. (USA). 2,2′-azoisobutyronitrile (AIBN) and Luria-Bertani agar (LBA) were purchased from Fluka (Germany). Ethyleneglycoldimethacrylate (EGDMA) was purchased from Fluka Biochemica (Switzerland). Elastin like polypeptide was produced and isolated from *E. coli* at the University of Valladolid, Spain. Tetracycline was a gift of Dr. I. Yılmaz of FAKO Ilac. San. (Istanbul, Turkey).

Methanol, acetic acid, sodium dodecylsulfate (SDS), 2-β-mercaptoethanol, isopropanol and glycerol were purchased from Merck (Germany). Glycine was purchased from USB (USA). Acrylamide was purchased from Amresco (USA). Ampicilline and isopropyl-β-D-thiogalactopyranoside (IPTG) were purchased from Apollo Scientific (UK). Luria–Bertani broth (LB) was purchased from Pronadisa (Spain).

Triton®X-100 was purchased from Applichem (USA). Fetal calf serum (FCS) was purchased from PAA (Austria). Dulbecco's Modified Eagle Medium (DMEM; high glucose) and Terrific Broth (TB) were purchased from Gibco (USA). Colorless DMEM (without sodium pyruvate and phenol red) was purchased from HyClone® (USA). Alamar Blue was from Biosource (USA). Alkaline Phosphatase 307 Kit was purchased from Randox® (UK). NucleoCounter reagents and nucleocasettes were purchased from Chemometec (Denmark).

2.2 Methods

2.2.1 Synthesis of pNIPAM

pNIPAM was synthesized by free radical polymerization method [122,123] with EGDMA as the crosslinker and AIBN as the photoinitiator under the presence of ultraviolet (UV) light. AIBN (1.36 mol % w.r.t. NIPAM), NIPAM (50% w/v) and EGDMA (1.2 mol % w.r.t NIPAM) were dissolved in isopropanol (polymer E). Different groups of polymers were obtained also by the addition of water in the last step in the ratios of 1:1 (polymer A), 3:7 (polymer C), 1:9 (polymer D) with respect to isopropanol. Another polymer group (polymer B) was synthesized doubling the crosslinker amount (2.4 mol % w.r.t NIPAM) without the addition of water. One last polymer group (polymer A*) was also synthesized by decreasing mol % of initiator, AIBN, to 0.3 with respect to NIPAM in a solvent mixture of 1:1 isopropanol/water. The feed composition ratios for the reactions are summarized in Table 1.

N_2 gas was bubbled through the reaction mixture for 10 min to remove oxygen dissolved in the reaction mixture. The reaction mixture was then poured into a petri dish, sealed with parafilm and put in a closed chamber. After an additional purge with N_2 gas for 5 min, the container was completely sealed with parafilm and kept under UV light for 6 h. The polymer was washed for several days with several distilled water changes to remove all the residues of unreacted monomer and other chemicals.

The polymer used as cell carrier *in vitro* in this study was polymer A*.

22

Table 1. Feed composition for the preparation of pNIPAM hydrogels

	Polymer A	Polymer B	Polymer C	Polymer D	Polymer E	Polymer A*
NIPAM	500 mg	500 mg	500 mg	500 mg	500 mg	500 mg
AIBN	10 mg	10 mg	10 mg	10 mg	10 mg	2.2 mg
EGDMA	10 µL	20 µL	10 µL	10 µL	10 µL	10 µL
Isopropanol	500 µL	500 µL	700 µL	900 µL	1 mL	500 µL
Water	500 µL	500 µL	300 µL	100 µL	——	500 µL

2.2.2 Preparation of pNIPAM Films

In order to prepare unpatterned pNIPAM films, the synthesis in section 2.2.1 was carried out in glass petri dishes with a smooth surface.

Patterns were created on the films by placing silicon wafers (groove width: 2 micrometer, ridge width: 10 micrometer, depth: 20 micrometer, angle: 54.7°) at the bottom of the petri dishes before introducing the reaction mixture. The synthesis was carried out under the same conditions.

2.2.3 Production and Isolation of ELP

The design of "ELP-RGD8" oligopeptide sequence and the molecular biology techniques that were used to clone the desired gene into expression vectors and transform *E. coli* BL21 strain were performed by Prof. J. Carlos Rodríguez-Cabello's group (BIOFORGE), at the University of Valladolid, Spain [34].

2.2.3.1 Inoculum Preparation

100 mL TB and 100 µL ampicillin (100 mg/mL) were put in an erlenmeyer. Two colonies of *E. coli* on LBA carrying the designed gene were transferred to the erlenmeyer containing TB with the aid of a sterile toothpick by gently touching on the colony and then putting it into the TB. This process was carried out in a laminar flow cabinet (Cruma, 870-FL, Spain). The erlenmeyer

was put in rotary shaker (Thermo Electron Corporation, 420 Incubated-Tabletop, USA) at 37°C for at least 16 h.

2.2.3.2 Growth of *E. coli* and ELP Production

LB or TB were autoclaved (Raypa, AES-28, Spain) before inoculation. Transformed *E. coli* were grown both in batch culture in a rotary shaker (Thermo Electron Corporation, 420 Incubated-Tabletop, USA) at 37°C and using a fermenter (2L) (B. Braun Biotech International, Biostat, Germany), in which temperature, pH, and oxygen levels were controlled and adjusted. Gene expression was induced by IPTG (0.8 mM) addition at an OD_{600} of 0.8 (Milton Roy Company, spectronic 601, USA). The cultures were incubated for an additional 3 h after induction.

2.2.3.3 Isolation of ELP from *E. coli*

The cultured cells were cultivated and centrifuged (Eppendorf, 5804 R, Germany) at $18x10^3$ g for 5 min at 4°C. The pellet was washed with Tris Buffered Saline (TBS, pH 8) (100 mL/L cell suspension) twice and centrifuged again at $18x10^3$ g for 5 min at 4°C. The pellet was resuspended in Tris-EDTA (TE, pH 8) solution (25 mL/L culture fermentation medium) and phenylmethylsulphonyl fluoride (PMSF) was put to avoid polymer proteolysis due to the activity of proteases and then the cells were lysed by sonication for 10 min with pauses of 2 s each 5 s at 100 W (Misonix, Sonicator 3000 USA). All these steps were carried out on ice. The lysate was centrifuged again at $18x10^3$ g for 5 min at 4°C. The supernatant which contains the total soluble proteins was collected and acidified to a pH value of 3 using 1.6 M HCl on ice. The proteins which become insoluble at this pH precipitated and they were removed by centrifugation at $18x10^3$ g for 5 min at 4°C. The supernantant's pH was changed to 10 using NaOH and it was warmed to 70°C for 1 h. ELP-RGD became insoluble at this temperature and precipitated by centrifugation at $18x10^3$ g for 5 min at 40°C. The pellet was dissolved in Milli-Q water (Millipore, USA) (1-2 mL/L culture fermentation medium) by stirring (IKA, Color Squid IKAMAG, Germany) at 4°C overnight. The protein solution was centrifuged at $15x10^3$ g for 20 min at 4°C. The supernatant was warmed to

24

70°C and the protein precipitated at this temperature was centrifuged again at 18×10^3 g for 5 min at 4°C. The final pellet was resuspended in cold Milli-Q water (0.5 mL/L culture fermentation medium) and freeze dried for at least 48 h (Labconco Corporation, FreeZone 1 Liter Benchtop Freeze Dry System, USA).

2.2.3.4 Determination of Protein Expression

Sodium dodecyl sulfate-polyacrylamide gel electrophoresis (SDS-PAGE) was performed using cell suspensions taken from the cell culture at different time points to evaluate protein expression profile of E. coli. It was also used for the evaluation of purification steps for ELP-RGD8 protein. The reagents of SDS-PAGE gel can be seen in Table 2.

Table 2. Reagents and Composition of SDS-PAGE gels

	Separating (Running) Gel		Stacking Gel
	10%	12%	4%
Acrylamide (40%)	2.5 mL	2.25 mL	500 µL
1M Tris pH 8.8	3.75 mL	2.8 mL	_____
0.5M Tris pH 6.8	_____	_____	1.25 mL
Milli-Q water	3.5 mL	2.25 mL	3 mL
SDS (10%)	75 µL	75 µL	50 µL
Ammonium Persulfate (APS) (10%)	50 µL	50 µL	50 µL
TEMED	5 µL	5 µL	12.5 µL

When the separating gel reagents were mixed, the solution was poured quickly into the gel cassette (Amersham Pharmacia Biotech, MiniVe, UK), leaving some space for stacking solution. In order to have a flat surface, a few drops of butanol was added carefully at the top of the gel and the gel was left to polymerize for 40 min. Stacking gel reagents were mixed leaving out APS

and TEMED until the gel was ready to be poured. Butanol was washed out before pouring the stacking gel solution. Since stacking gel polymerizes very quickly, the comb to form wells for loading was placed immediately after pouring the stacking gel on the separating gel avoiding making bubbles underneath the comb. The gel was left to polymerize for an aditional 20-30 min.

Cell suspensions taken at different time points during culture were collected in 1.5 mL Eppendorf tubes and centrifuged (Eppendorf, MiniSpin, Germany) at $13.4x10^3$ rpm. The pellets were stored at 4°C until SDS-PAGE was performed. Then they were resuspended in TBS (pH 8) and mixed with sample buffer (3X) at a ratio of 4:1. Sample buffer (3X) was composed of 3mL of 0.5 M Tris (pH 6.8), 2.4 mL of glycerol, 4.8 mL of 10% SDS, 1.2 mL of 2-β-mercaptoethanol and 15 µL of 2% Bromophenol Blue. The gel cassette was clamped into the electrophoresis apparatus and the buffer chambers were filled with 1X running buffer (also named as Laemmli buffer) (pH 8.3). Running buffer (5X) was composed of 15 g of Tris base, 72 g of glycine and 5 g of SDS in 1 L of water. The samples were boiled for 5 min and 5-7 µL of the samples were loaded in seperate wells of the stacking gel. The gels were run at 300V for about 2 h (Amersham pharmacia biotech, EPS301 Power Supply, UK). The gels were stained in Coomassie-Blue staining solution (0.1% Coomassie Blue, 10% acetic acid, 40% methanol) for overnight on a rocking shaker in slow mode (Heidolph, Duomax 1030, Germany). To eliminate unspesific binding of the stain, the gels were immersed in Coomassie-Blue destaining solution (10% acetic acid and 40% methanol) or in hot water for hours long on the shaker with several changes, until the gel becomes destained. The gels were monitored and gel photos were taken by "Gel logic 100 Imaging System" (Kodak, USA) and analysed by "Kodak 1D Image Analysis Software".

2.2.4 Adsorption of ELP-RGD6 on pNIPAM Films

ELP-RGD6 was a gift from Prof. J. Carlos Cabello-Rodríguez, University of Valladolid, Spain. The protein was dissolved in distilled water at a concentration of 0.1% (w/v). The solution was filter sterilized with 0.2 µ pore

sized syringe filters (Orange Scientific). Dry pNIPAM films were sterilized by UV for 30 min at each side. 100 μL of this solution was put on patterned and unpatterned pNIPAM films and left to dry in a laminar flow hood (LaminAir Safe 2000, Holten A/S, Denmark) for 2 days.

2.2.5 Characterization of pNIPAM Films:

2.2.5.1 Microscopic Examination

2.2.5.1.1 Scanning Electron Microscopy (SEM)

Patterned and unpatterned pNIPAM films were gold coated under vacuum and micrographs were taken with a Scanning Electron Microscope (SEM) (FEI QUANTA 400-F, Holland) in (Central Laboratory, METU).

2.2.5.2 Water Contact Angle Measurement

Unpatterned pNIPAM films were incubated at 29°C and 37°C for 48 h. The excess water on the surface of the films was absorbed by gently touching a tissue paper to the surface. Water contact angle measurements were performed using a goniometer (CAM 200, KSV Ltd, Finland).

2.2.5.3 Swelling of pNIPAM Films versus Temperature

The swelling behavior of polymer discs at various temperatures was studied by weighing the polymer discs at 20-37°C after equilibrating the samples in a temperature controlled water bath. At each particular temperature, samples were incubated in distilled water for 24 h, wiped with moistened filter paper to remove excess water from the sample surface, and weighed.

2.2.6 *In vitro* Studies:

2.2.6.1 Isolation of Bone Marrow Stem Cells (BMSCs) from Rat

Six week old male Sprague-Dawley rats weighing approximately 150 g were euthanized and disinfected with 1:1 (v/v) betadine-70% EtOH. Surgery took place in the laminar flow hood under aseptic conditions.

The femur and tibia were excised and placed in 50 mL Falcon tube containing the harvest medium (100 units/mL penicillin, 100µg/mL streptomycin in high glucose Dulbecco's Modified Eagle Medium (DMEM)). Bones were then transferred to sterile petri dishes with harvest medium. The soft tissue covering the bones was removed with the help of sterile surgical blades and metaphyseal ends of the femur and tibia were cut off to enable access to the bone marrow. The needle of a sterile syringe containing 4 mL of primary medium (high glucose DMEM supplemented with 100 units/mL penicillin, 100 µg/mL streptomycin and 10% fetal calf serum (FCS)) was introduced into the femur and tibia midshafts and the bone marrow was put in 15 mL Falcon tubes. The bone marrow cell suspensions in 15 Falcon tubes were centrifuged for 5 min at 3000 rpm (RotaFix 32, Hettich Zentrifugen, Germany). The supernatants were discarded and the remaining pellets were resuspended with 2 mL of primary medium by the aid of 2 mL sterile pasteur pipettes. The cell suspensions were transferred to sterile T-75 tissue culture flasks and 8 mL of primary medium was added into each flask. The flasks were placed into a carbon dioxide incubator (5% CO_2, Sanyo MCO-17AIC, Japan) at 37°C and left undisturbed for 2 days to enable cell attachment. After 2 days, the medium was discarded and the cells were washed with phosphate buffered saline (PBS) (0.01M, pH 7.4). The medium was refreshed every two days. When the cells reached confluency, medium was discarded and the cells were washed 3 times with PBS (0.01M, pH 7.4) to remove FCS completely since it is known to inactivate trypsin. Trypsin-EDTA solution (0.05%, PBS diluted from 0.25% stock) was warmed to 37°C and 2 mL was added into the T-75 flasks. Then the cells were incubated for 3-4 min in the carbon dioxide incubator at 37°C. The detachment of cells was checked by light microscope. Primary medium containing 10% FCS at least 3 times the volume of trypsin

solution (0.5%) was added into the flasks to terminate trypsin activity. The cell suspensions were centrifuged for 5 min at 3000 rpm. The supernatant was discarded and the cells were resuspended in FCS. The number of cells was determined with a nucleocounter (Chemometec A/S Nucleo Counter, Denmark). In brief, 100 µL of cell suspension was taken into a 1.5 mL eppendorf tube and pumped into a nucleocasette. Then the nucleocasette was placed in the nucleocounter and the instrument gave the number of dead cells per mL of cell suspension. Another 100 µL of cell suspension was taken into a 1.5 mL eppendorf tube and mixed with Reagent A, which is a lysis buffer and then with Reagent B, which stabilizes the nucleus of the cells. This mixture was pumped into another nucleocasette and placed in the nucleocounter. This time the number given by the machine was the total cell number per mL of cell suspension and it was multiplied by the dilution factor, 3. The live cell number was calculated by subtracting the dead cell number from the total cell number and the number obtained was again multiplied by the volume (mL) of cell suspension. The cells in FCS were distributed to 2 mL cryovials and 10% dimethyl sulfoxide (DMSO) was added into each cryovial. Cell number/vial did not exceed $1x10^6$ cells/mL. Cryovials were placed into a freezing container (5100 Cryo 1°C Freezing Container, Nalgene, USA) immediately after the DMSO was added. The freezing container was left at -80°C in a deep freeze overnight. The following day, cryovials were transferred to the liquid nitrogen tank (-196°C).

2.2.6.2 Culture of BMSCs

Cryovials carrying frozen cells were taken out of the nitrogen tank and thawed quickly by holding in hand. The suspensions were diluted immediately by adding 8 mL primary medium for each 2 mL cell suspension and centrifuged at 3000 rpm for 5 min.

The precipitated cells were resuspended in 0.5 mL of primary medium for each cryovial. The cell number was determined with nucleocounter and the cells were seeded onto T-25 or T-75 flasks at a cell seeding density of $20x10^3$ cells/cm^2 and were incubated for about 1 week until they became confluent refreshing the medium every 2 days.

2.2.6.3 Cell Seeding on Films

The medium in the flasks was discarded and the cells were washed with PBS (0.01M, pH 7.4) 3 times. Warm (37°C) 0.05% trypsin-EDTA was added into each flask; 1 mL for T-25 and 2 mL for T-75 flasks. The cells were left in a carbon dioxide incubator at 37°C for 3-4 min. After their detachment was observed with the light microscope, primary medium containing 10% FCS at least 3 times the volume of trypsin solution (0.5%) was added into the flasks to terminate trypsin activity. The cells were centrifuged at 3000 rpm for 5 min to remove trypsin-EDTA containing medium and were resuspended again in 2 mL of primary medium. The number of viable cells was determined by using the nucleocounter. Then 20×10^3 cells were seeded onto each sterile, dry film which were placed in 24-well tissue culture plates conating 30 µL medium per well. The samples were incubated at 37°C for 3 h for attachment onto the films. After 3 h, 1 mL of differentiation medium composed of high glucose DMEM supplemented with 100 units/mL penicillin, 100 µg/mL streptomycin, 4% amphotericin B, 10% FCS, 10 mM β-glycerophosphate, 50 µg/mL L-ascorbic acid and 10 nM dexamethasone was added into each well. Medium in the well was changed every two days.

2.2.6.4 Dynamic culturing of the BMSCs

Tensile stress was applied to cells utilising the thermoresponsiveness of pNIPAM films. The swelling behavior of pNIPAM films synthesized with different solvent compositions and crosslinker percentages were studied. The polymer type used in the cell experiments consisted of AIBN (0.3 mol % w.r.t. NIPAM), NIPAM (50% w/v), EGDMA (1.2 mol % w.r.t. NIPAM) in isopropanol:water ratio of 1:1 (See Table 1).

Tension was generated on the pNIPAM films by changing the temperature to 29°C. The 24-well tissue culture plates carrying the cell seeded pNIPAM films were taken out of the carbon dioxide incubator at 37°C, placed into the laminar flow hood and the caps of the plates were left open for 5 min to achieve rapid temperature change. Then the caps were closed and the flasks were transferred to another carbon dioxide incubator maintained at 29°C (5%

CO_2) (Heal force HF90, Shangai Lishen Scientific Equipment Co., Ltd., China). After incubating at 29°C for 10 min, the plates were again transferred to the previous carbon dioxide incubator that was maintained at 37°C. Ten cycles of temperature switches between 37 and 29°C were applied 5 days starting on the second day post cell seeding.

2.2.6.5 BMSC Characterization on Films

2.2.6.5.1 Cell Proliferation Assay with Alamar Blue™

Alamar Blue assay was performed in order to investigate cell proliferation. Alamar Blue calibration curve was prepared for BMSC at passage 2 cultured in the primary medium. Different amounts ($1x10^4$, $2x10^4$, $5x10^4$, $7.5x10^4$, $10x10^4$, $15x10^4$, $17.5x10^4$, $20x10^4$) of BMSC were seeded on 24-well tissue culture plates in duplicate. The cells were incubated for 3 h for attachment on the TCP in carbon dioxide incubator at 37°C. After 3 h, the medium was removed and the wells were washed with PBS (10 mM, pH 7.4). 1 mL Alamar Blue solution (10% in colorless DMEM medium) was added into each well and the cells were incubated for 1 h in Alamar Blue solution in a carbon dioxide incubator at 37°C.

After 1 h, 200 μL of the Alamar Blue solution from each well was transferred into a 96-well tissue culture plate in triplicate. Their absorbances were measured at 595 nm and 570 nm by the Elisa Plate Reader (Maxline Vmax®, Molecular Devices, USA). Percent reduction of the dye due to the metabolic activity of the cells was determined by using the recommendations absorption coefficients of the reduced and oxidized dye according to the manufacturer's recommendation. A calibration curve of the reduction percentage of the dye versus viable cell number was constructed (*Appendix A*).

Alamar Blue assay was performed on Days 1, 7, 14 and 21 of culture. Cell seeded and unseeded films were transferred into other 24-well tissue culture plates and washed with PBS (10mM, pH 7.4). Alamar Blue solution (1 mL, 10% in colorless DMEM medium) was added onto each well and the cells were incubated for 1 h with Alamar Blue solution in a carbon dioxide incubator at

37°C. All solutions introduced to cells were preheated to 37°C in order to eliminate polymer swelling.

After 1 h, 200 µL of the Alamar Blue solution from each well was added into a 96-well tissue culture plate in triplicate and their absorbances were measured at 595 nm and 570 nm by the Elisa Plater Reader. The films without cells were used as blank controls. The films were washed twice with PBS (10 mM, pH 7.4) to remove the Alamar Blue to a large extent, and then they were transferred again to their original 24-well tissue culture well plates in which they were seeded. 1 mL of differentiation medium was added into each well for continuity of culture.

The absorbance values were analyzed according to the manufacturer's recommendation and the viable cell numbers were determined using the previously prepared calibration curve for BMSC (*Appendix A*).

2.2.6.5.2 Assessment of Cell Differentiation with ALP Assay

Alkaline phosphatase (ALP) assay was performed for cell seeded films, unseeded films and TCP cultured for 7, 14 and 21 days. At these time points, the medium inside the wells was removed and the films were washed with PBS (10 mM, pH 7.4). The films were cut and transferred into 15 mL Falcon tubes containing 500 µL of Tris Buffer (10 mM, pH 7.5, 0.1% Triton®X-100) to lyse the cells. They were stored at -20°C until the assay was performed. On the day of the assay, films in the lysis buffer were thawed in a carbon dioxide incubator at 37°C and then frozen at -20°C to ensure complete lysis and this cycle was repeated three times. Then each sample was sonicated for 5 min at 25W (Ultrasonic Homogenizer, Cole Parmer, USA) on ice with 30 s on, 30 s off cycles, for a total of 9.5 min. Before sonication the Falcon tubes containing the films were incubated in a water bath at 37°C for 1 min in order to remove the fluid inside the films. After sonication the same method was used (incubation at 37°C in water bath) for 5 min and then the films were taken out of the solution. The cell lysates were then centrifuged at 2000 rpm for 10 min. Supernatants of each sample were collected in different 1.5 mL eppendorf tubes. 10 µL of each supernatant was added to 240 µL of substrate

(p-nitrophenyl phosphate reconstituted with $MgCl_2$-diethanolamine buffer supplied by Randox AP307 kit). The time dependent absorbance of the mixture was obtained at 405 nm every min for a total of twelve min by Elisa Plate Reader (readings were performed in duplicate). In case there was not a significant colorimetric change, the amount of supernatant used was increased to 100 µL and the volume of substrate was decreased to 150 µL. Graph of optical densities at 405 nm (OD_{405}) vs. time was drawn for each sample and the slopes were calculated. The data was analyzed by using the slope of the calibration curve previously prepared with p-nitrophenol (*Appendix B*) to determine enzyme activity in units of nmol substrate converted to product/min.

ALP activity (nmoles/min/sample) was calculated as follows:

Net OD_{405} = $OD_{405, \text{ seeded film}}$ − $OD_{405, \text{ unseeded film}}$

Slope of Net OD_{405} vs. Time graph = Net OD_{405}/ min for sample

Slope of calibration curve = OD_{405} /nmoles of p-nitrophenol

ALP Activity (nmoles/min/sample) = [(Net OD_{405}/min for sample) / (OD_{405} /nmoles of p-nitrophenol)] x (Total volume of lysis buffer (µL) / Amount added on the substrate (µL))

Also specific ALP activity (ALP activity/cell) was calculated for each sample dividing the total ALP activity per sample to the number of the cells determined by Alamar Blue assay on the day the ALP assay was performed.

2.2.6.5.3 Determination of Mineralization

2.2.6.5.3.1 Fluorescence Microscopy

To detect mineralization on the films, differentiation medium containing 10 µg/mL tetracycline instead of 100 units/mL penicillin and 100 µg/mL streptomycin was given to cells beginning from the 3rd day of culture. Tetracycline is known to bind to calcium and it is autofluorescent. On Day 21 of culture, the cells were washed with PBS (10mM, pH 7.4), twice with 70% ethanol and fixed in 96% ethanol at 37°C for 6 h [124]. The ethanol was discarded and the films were left to dry wrapped in aluminium foil to keep in

dark. Mineralization was observed using a fluorescence microscope (Leica, DFC 300 FX, Germany) at 480 nm.

2.2.6.5.3.2 SEM Examination

On Day 21 of culture, cells were fixed with glutaraldehyde (2.5% glutaraldehyde in 0.1M, pH 7.4 sodium cacodylate buffer) for 2 h. After fixation, they were washed three times with cacodylate buffer with 30 min incubation periods to ensure complete removal of glutaraldehyde. All solutions introduced to cells were preheated to 37°C in order to eliminate polymer swelling. The samples were frozen at -80°C over night and freeze dried the following day, for 10 h under 4.5×10^{-2} mbar pressure. The dry samples were gold coated under vacuum and then examined by Scanning Electron microscope (SEM) (FEI QUANTA 400-F, Holland) (Central Laboratory, METU). The whole surfaces of the films were also scanned with X-ray photoelectron spectroscopy (XPS) and percentage of calcium and phosphate elements were found.

CHAPTER 3

RESULTS AND DISCUSSION

3.1 Characterization of Films

3.1.1 Swelling of pNIPAM Films

Temperature responsiveness studies were performed by weighing the polymer discs at different temperatures (20-37°C) and swelling behavior at different temperatures was studied (*Fig.* 4 a). The water content of polymer discs at different temperatures were calculated by subtracting the weight of dry polymer (W_d) from the weight of swollen polymer (W_s) after it was incubated at a particular temperature in water bath for 24 h ((W_s-W_d)/W_d (g water/ g dry gel)).

All polymer groups showed similar swelling behavior between 37 and 34°C, but a sharp transition was observed between 34 and 31°C, which is the range in which the LCST (~32°C) of pNIPAM (*Fig.* 4). The only exception was polymer B. This was an expected result because of the relatively high crosslinking degree of polymer B. The crosslinker amount significantly affected the swelling behavior; increased crosslinker content of the reaction mixture resulted in decreased swelling behavior, especially below 31°C. At 20°C, the water content of polymer A was twice that of polymer B, which was synthesized in the presence of crosslinker twice as much than in the synthesis of polymer A.

The amount of initiator in the reaction mixture did not have effect on LCST and swelling behavior of the polymer A (*Fig.* 4 b).

(a)

(b)
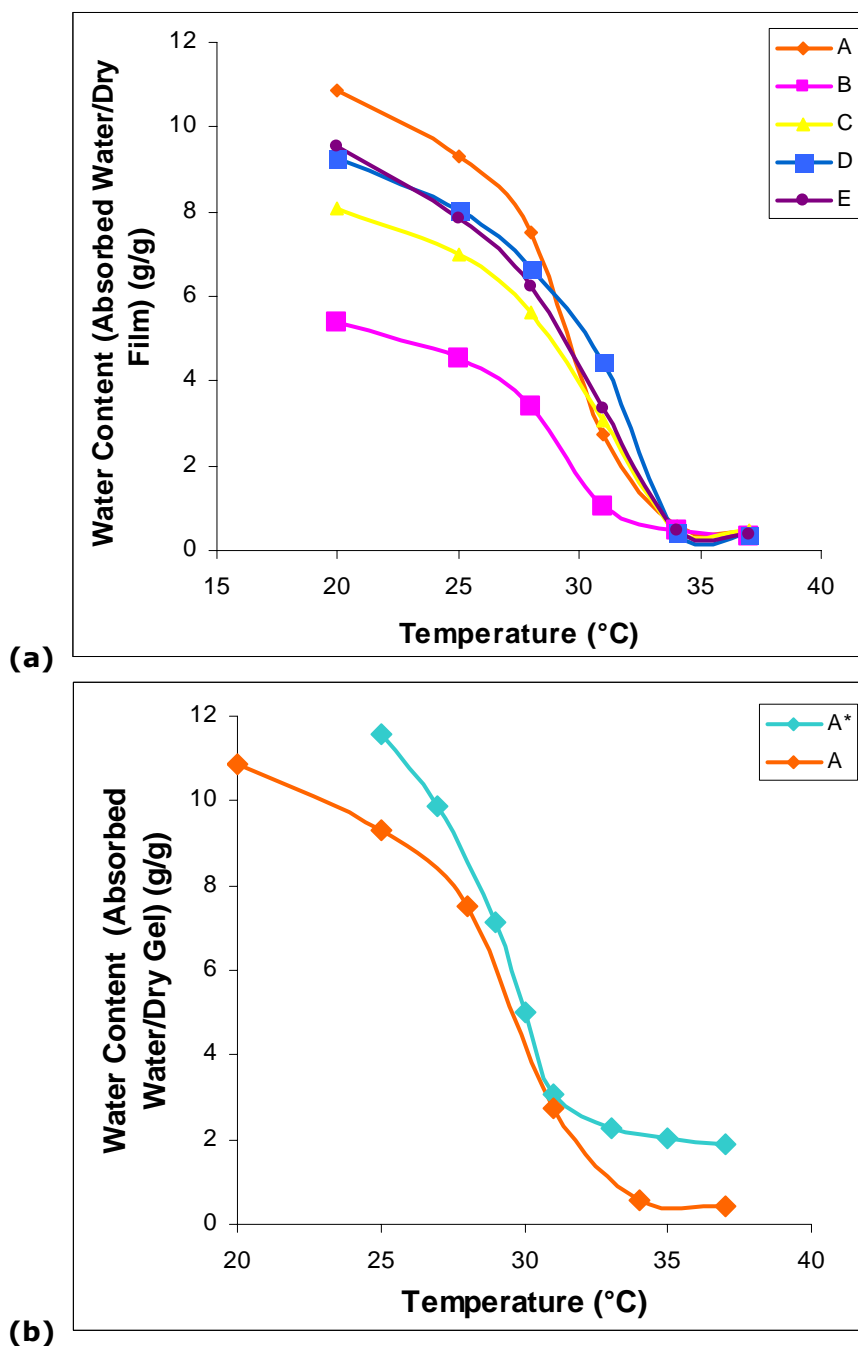
Figure 3. Swelling of polymers (a) prepared with different solvent mixtures and crosslinker amounts:
A = 0.5 g/mL NIPAM in 2-Propanol : water = 1:1
B = 0.5 g/mL NIPAM in 2-Propanol : water = 1:1
C = 0.5 g/mL NIPAM in 2-Propanol : water = 7:3
D = 0.5 g/mL NIPAM in 2-Propanol : water = 9:1
E = 0.5 g/mL NIPAM in 2-Propanol

(b) Swelling of polymer A (AIBN: 1.36 mol % w.r.t NIPAM) and A* (AIBN: 0.3 mol % w.r.t. NIPAM)

3.1.2 Water Contact Angle Measurement

After an incubation of 48 h at 29°C and 37°C, water contact angles of unpatterned pNIPAM films (A*) were measured using a goniometer. The water contact angle was measured as 60.5° ± 5.3 at 37°C and 21.0° ± 5.7 at 29°C. This finding indicates a significant increase in hydrophilicity upon temperature decrease, and explains the reason of swelling at temperatures below the LCST.

3.1.3 Calculation of Strain Applied to BMSCs Under Dynamic Conditions

pNIPAM films were prepared ultimately to use as a cell carrier with a capacity of generating tension on BMSCs, seeded on the films, through temperature changes to study the effect of dynamic tensile stress on BMSCs (proliferation, alkaline phosphatase activity, mineralization). The conditions of dynamic culturing were presented in section 2.2.5.4. Briefly, pNIPAM films carrying the cells were incubated in a carbon dioxide incubator at 37°C, transferred to a laminar flow cabinet and the caps of the plates were left open for 5 min to achieve rapid cooling, then they were transferred to another carbon dioxide incubator maintained at 29°C and left there for 10 min. Finally the cells were again transferred to the original incubator at 37°C and kept there for 30 min. Ten cycles of temperature switches (37-29-37°C) were applied per day for 5 days starting on the second day post cell seeding. Three unpatterned pNIPAM films were incubated under the same conditions in PBS (10 mM, pH 7.4) just to measure the elongation and contraction of films upon temperature changes. Strain was calculated by the equation below:

$$\varepsilon = \frac{\Delta L}{L_0} = \frac{\left| L - L_0 \right|}{L_0} \tag{3.1}$$

where; ε is the strain in measured direction, L_0 is the original length of the film, L is the current length of the film.

The percentage strain calculated using the 3 unpatterned pNIPAM films were varying between 2.2 and 10%, with an average of 5.9% (± 2.3%). The deviation in the elongation values might be the result of the not so precisely controlled temperature change which took place in the laminar flow hood. Also, it is important to note that polymers were not synthesized at the same date.

Strain is a dimensionless unit. 1 strain is defined as 100% elongation. 0.1%, which is equivalent to 1000 µstrain, is in the physiological range in loaded bone tissue [125]. Strain magnitudes between 1000 and 10000 µstrain were reported to occur in the gap of fracture site of healing bone [126]. In comparison to these, the mechanical strain generated by pNIPAM films under the defined conditions in this study was in a high magnitude range.

3.1.4 Microscopic Examination

The surface characterization of the synthesized polymer films were done by microscopy.

3.1.4.1 SEM

SEM micrographs of cell seeding surfaces of patterned and unpatterned films (A*) presented in Figures 14 A and 14 B show that the pattern could be transferred with high fidelity onto the polymer. Figure 14 C shows the unpatterned film with the same chemistry with the others.
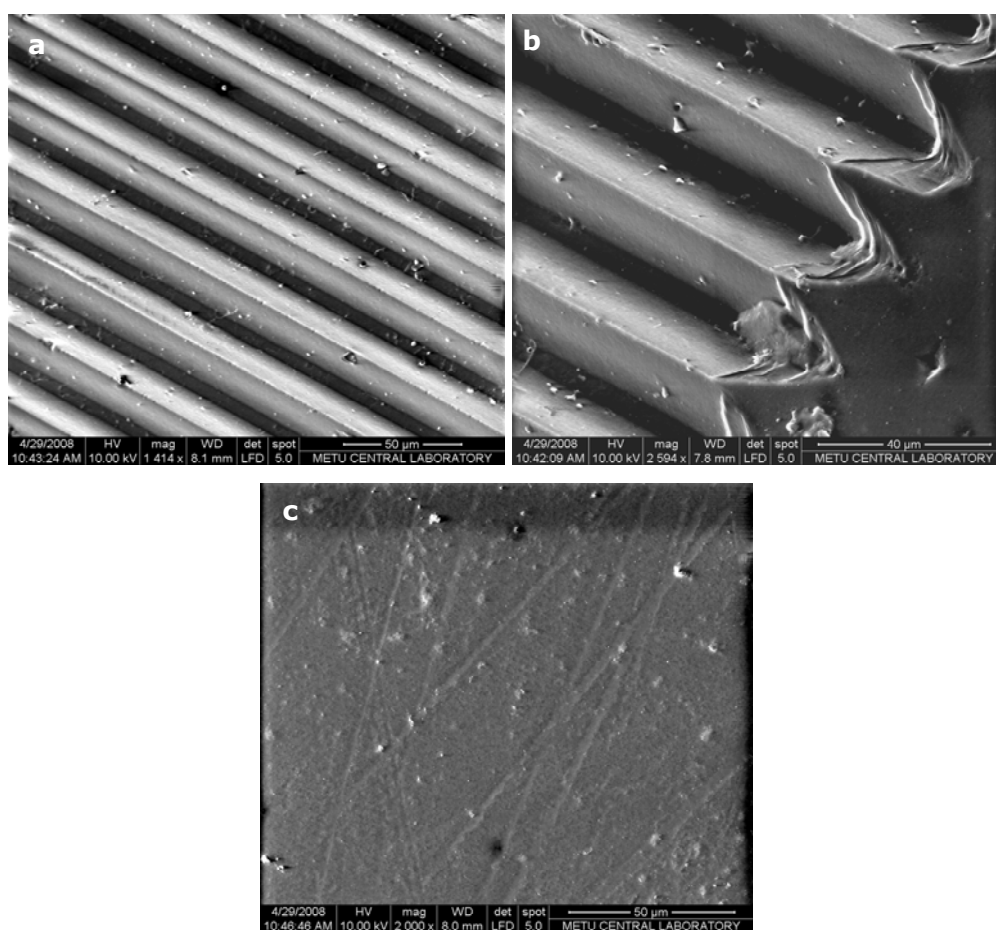
Figure 4. SEM images of pNIPAM films of type A* (a) Patterned pNIPAM film, from edge (x 2504), (b) patterned pNIPAM film, (x 1414), (c) unpatterned pNIPAM film, (x 2000).

3.2 Determination of Protein Expression and Isolation of ELP-RGD8

E. coli BL21 strain, which were transformed to carry ELP-RGD8 gene, was grown both in batch culture on a rotary shaker at 37°C and using fermentor. Gene expression was induced by addition of IPTG (0.8 mM) at an OD_{600} of 0.8, which corresponds to the exponential growth phase. The cultures were incubated for an additional 3 h after induction. These steps were optimized by Prof. J. Carlos Rodríguez-Cabello's group (BIOFORGE), at the University of Valladolid, Spain.

SDS-PAGE was performed to determine the protein expression in *E. coli*. SDS-PAGE is a technique used to separate proteins based on their size, which correlates with their molecular weights. SDS is an anionic detergent which denatures proteins and also applies a uniform negative electrical charge to each protein in proportion to its mass. Without SDS, proteins with similar molecular weights would migrate differently in the gel due to the differences in their mass to charge ratios. Therefore, SDS eliminates the effect of differences in shape so that chain length is the only determinant of the migration rate of proteins under the influence of an applied electric field. The rate of mobility in the gel depends on the pore size of gel, a property which can be modified by adjusting the concentration of acrylamide and the crosslinker, and the magnitude of the electric field applied. Proteins with lower molecular weights migrate more quickly through the pores of gel than those with higher molecular weights.

For the isolation of ELP-RGD8, cell lysates were prepared by breaking cell membranes by sonication, releasing the proteins. PMSF, protease inactivator, was added prior to sonication to prevent ELP-RGD8 degradation. The cell debris was precipitated by centrifugation and the supernatant containing the total soluble proteins was acidified to a pH value of 3. ELP-RGD8 was soluble at this pH and after centrifugation, the acidified supernatant carried the ELP-RGD8 (*Fig.* 6 lane 2), whereas the precipitate did not (*Fig.* 6 lane 1).
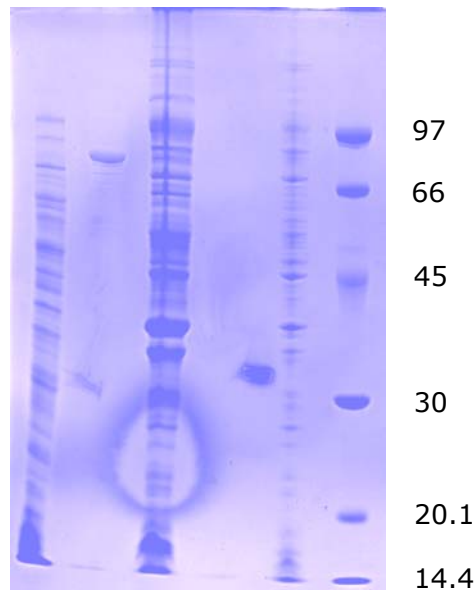
Figure 5. SDS-PAGE image of *E. coli* proteins and ELP-RGD. Lane 1 shows precipitate and lane 2 shows supernatant of centrifugation at pH 3. Lane 3, the pellet of sonication; lane 4, O/N culture in fermentor 2 h after induction; lane 5, O/N culture in fermentor just after induction; lane 6, molecular marker (kDa).

Later, the pH of the supernantant was increased to 10. This pH value is specific for ELP-RGD8 purification. All lysine residues in the protein are neutralized at pH 10. Also, for an efficient precipitation of this protein at this pH value, the temperature needs to be above the transition temperature of the protein (~33°C) (*Fig.* 7 Lane 5).
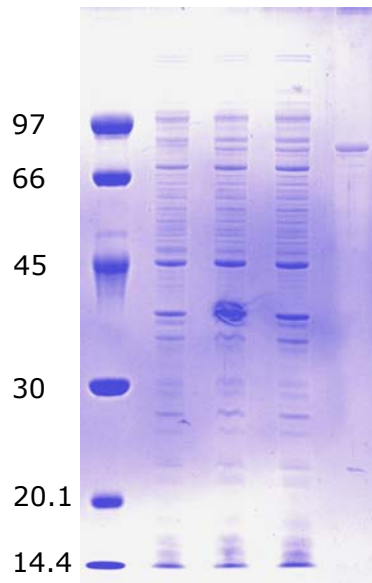
Figure 6. SDS-PAGE image of E. coli proteins and ELP-RGD. Lane 5 shows precipitated ELP-RGD8 at pH 10, 70°C. Lane 1, molecular marker (kDa); lane 2, TB batch culture just after induction; lane 3, TB batch culture 1 h after induction; lane 4, TB batch culture 3 h after induction.

The precipitated ELP-RGD8 was dissolved in Milli-Q water by stirring at 4°C overnight. The protein solution was subjected to a series of cold (4°C)-hot (70°C) centrifugation, and the final pellet was freeze dried.

3.3 In vitro Studies

3.3.1 Cell Proliferation

A calibration curve was constructed by seeding different amounts (1×10^4, 2×10^4, 5×10^4, 7.5×10^4, 10×10^4, 15×10^4, 17.5×10^4, 20×10^4) of BMSCs at passage two on 24-well tissue culture plates in duplicate and determining the viable cell number with the Alamar Blue assay (*Appendix A*).
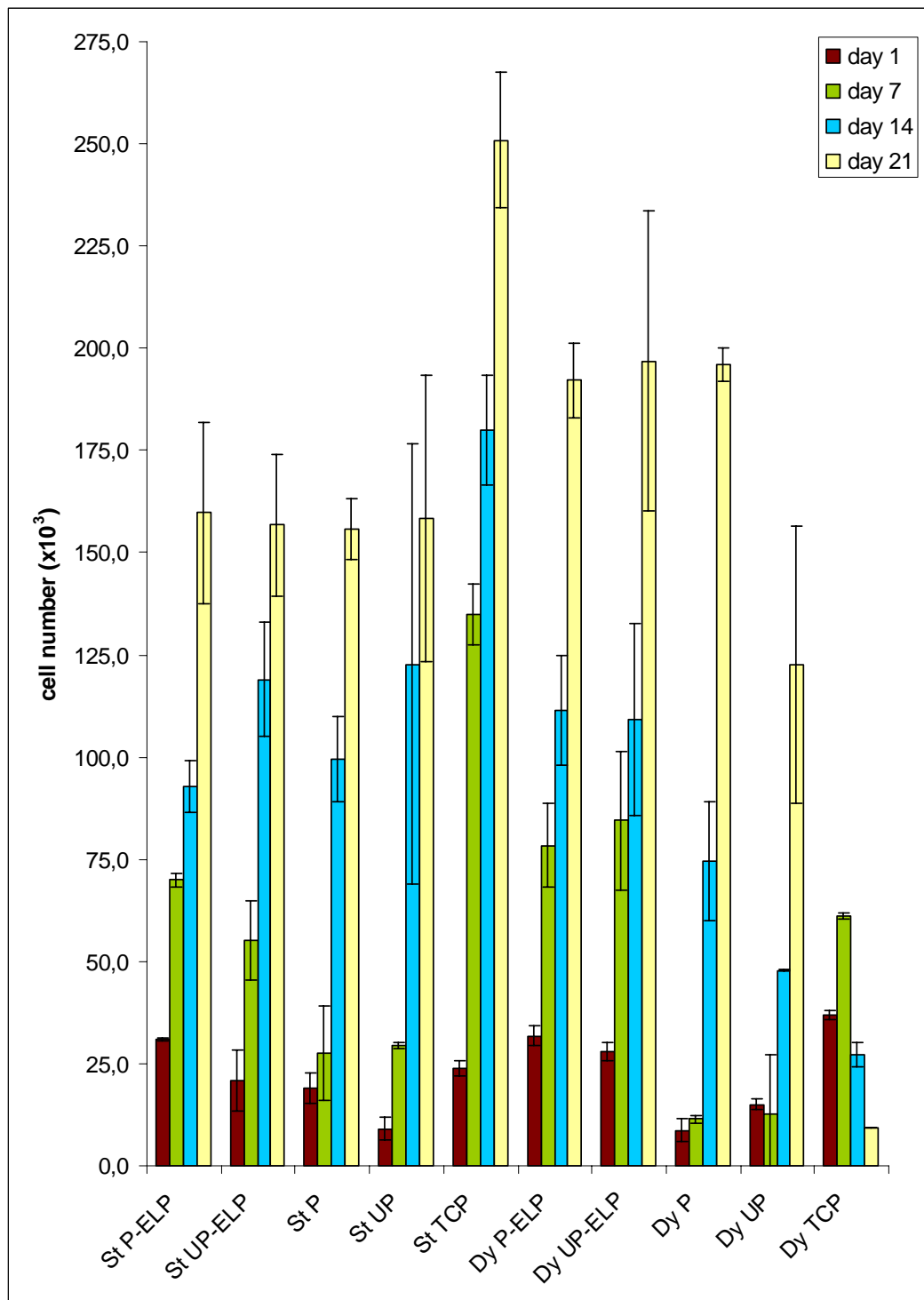
Figure 7. Cell proliferation on the pNIPAM films with different surface topography and chemistry under static and dynamic conditions, and on TCP. (St: static, Dy: dynamic, P: patterned, UP: unpatterned, P-ELP: patterned and ELP adsorbed, UP-ELP: unpatterned and ELP adsorbed)

Cell numbers were determined on Day 1, 7, 14 and 21 of culture on the samples of TCP, unpatterned and patterned pNIPAM films with and without adsorbed ELP, cultured under static and dynamic conditions (*Fig.* 8).

Although the cell number seeded on each film and the control TCP was $20x10^3$, the 1st day poliferation results showed that the cell numbers on the samples varied between $8.8x10^3$ which is on Dy P and $37x10^3$ which is on Dy TCP. The low level of cell number can be explained by insufficient attachment but 2-fold high number cannot be explained by cell division because the time for cell division is 48-72 h [127]. This may be explained by an error that occured during cell dispensing. It is also important to note that on the first two days post cell seeding, all samples were cultured in static conditions (in incubator at 37°C, 5% CO_2), so there should not have been a difference between the unpatterned and patterned pairs. However it can not be stated that the initial cell attachments occured randomly because consistently the cell numbers were more on ELP adsorbed films (St P-ELP, St UP-ELP, Dy P-ELP, Dy UP-ELP) and on TCP (St TCP, Dy TCP) than films without any protein modification on the surface (St P, St UP, Dy P, Dy UP). This result was expected because the protein ELP used in this experiment was genetically modified to include the cell adhesive RGD (arginine-glycine-aspartic acid) amino acid sequences. This result also demonstrated that the adsorption of ELP on films was successful.

One week results showed that the cell numbers on ELP adsorbed films were still higher than those on the films without ELP under static culture. However, when the cell number increase (%) in Figure 9 for day 1 to 7 is studied, a higher increase in cell number was seen on the St UP films than St P-ELP and St UP-ELP. The highest increase in cell number was on St TCP and the lowest increase was on St P at the end of the first week. It is interesting that although the 1st day cell number on St P films ($18.9x10^3$) was twice as much as the cell number on St UP films ($9.1x10^3$), increase in cell number on St P films was just 46% whereas increase in cell number on St UP films was 225%. This relatively low increase in cell number on St P films can be explained by the possibility of aggregate formation of cells and subsequently leaving the film surface.

Proliferation rate of the cells were expected to decrease with time due to increased osteogenic activity upon down regulation of cell proliferation [128]. The cells on St P-ELP and St UP-ELP followed this fashion and their proliferation rates decreased, on the other hand the cells on St P and St UP continued to increase their numbers. On day 14 of culture, the difference of cell numbers on the films was not significant, except St P-ELP and St UP-ELP.

The cell numbers on the films of static group were almost the same on the 21st day of culture and the highest cell number was observed on St TCP, being 1.6 fold of those on St P-ELP, St UP-ELP, St P and St UP.
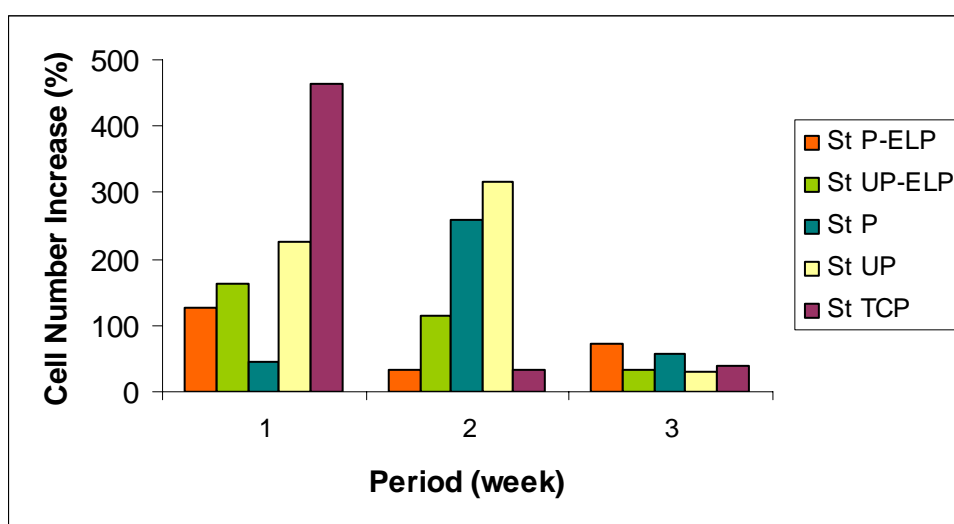
Figure 8. Increase in cell number when cultured under static conditions.

The dynamic conditions were generated by cyclic temperature change between 37 and 29°C utilising the thermoresponsiveness of the pNIPAM films (altering their dimensions upon temperature change). Ten cycles of temperature switches were applied for 5 days beginning from the second day post-cell seeding between 37 and 29°C. Duration of these cycles was 15 min at 29°C and 30 min at 37°C.

The cell numbers on Dy P-ELP and St P-ELP was close and Dy UP-ELP was significantly higher than St UP-ELP at the end of the first week. However the cell numbers on the films that were not ELP adsorbed (Dy P, Dy UP) increased very few (Dy P: 30.5 %) or decreased (Dy UP: 15.1 %) (*Fig.* 10). This result was not surprising because when the temperature is below lower critical solution temperature (LCST), which is around 32°C, pNIPAM becomes hydrophilic leading to weakened cell attachment. Okano et al. (1990) [90] used this property to detach cells from temperature responsive culture dishes that were pNIPAM grafted and obtained cell sheets eliminating the need for trypsin or cell scrapers. On the other hand, at 37°C, which is above the LCST, cells can attach and proliferate on pNIPAM. Once more the effect of ELP on cell attachment was observed and it can be stated that the cells cultured under dynamic conditions retain themselves in attached form on the surface in the presence of ELP.
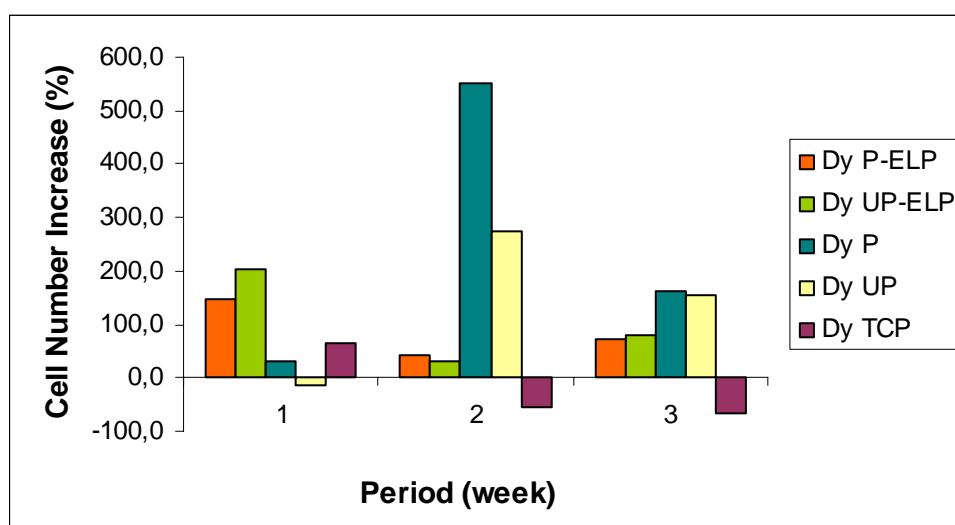
Figure 9. Increase in cell number when cultured under dynamic conditions.

After the cells were subjected to dynamic loading for five days, they were kept under static conditions (in incubator at 37°C, 5% CO_2) beginning from the 7th day of culture until 21st day.

46

After two weeks, the cell numbers on Dy P-ELP and Dy UP-ELP were very close to each other and also to all the groups under static culture except St TCP. The highest increase in cell number between day 7 and 14 was on Dy P films and the number of cells were not significantly lower than the number of cells on Dy UP-ELP films. The second highest increase in cell number was seen on Dy UP films for the same period of time but the cell number was still lower than the cell numbers on Dy P-ELP and Dy UP-ELP films.

On the 21st day, still the cell number increase was higher on films without ELP (Dy P and Dy UP) than ELP adsorbed films (Dy P-ELP and Dy UP-ELP). The number of cells on Dy P-ELP, Dy UP-ELP and Dy P were almost the same and the number of cells on Dy UP is not significantly lower than Dy UP-ELP but significantly lower than Dy P-ELP and Dy P.

The cells which were subjected to cyclic mechanical load as a result of cyclic temperature changes for five days continued to proliferate and reached comparable cell numbers to those on the films of static group. On the other hand although the 1st day cell number on Dy TCP was 1.5 fold of cell number on St TCP, at the end of the first week the cells on St TCP increased in number by 463% of the 1st day becoming 2.2 fold of cell number on Dy TCP. Moreover after the first week of culture, cell number on Dy TCP started to decrease and on the 21st day the lowest cell number was on Dy TCP (9.2×10^3) which is 0.2 fold of the cell number on Dy TCP at day 1 (37×10^3) and 0.04 fold of the cell number on St TCP at day 21 (250.9×10^3). The decrease in cell number on Dy TCP can be ascribed to the cyclic temperature changes. The cells on the films in dynamic group were also under the same conditions (10 cycles of 29°C for 15 min and 37°C for 30 min a day, continued for 5 days post cell seeding) with the cells on TCP, therefore they were also subjected to the same adverse effects of temperature change. But the only difference between the cells on TCP and on films was the mechanical stress created by the films. So this finding shows that the effect of mechanical stress created under the conditions is the enhancement of proliferation of cells and compensation of the adverse effect of temperature change.

3.3.2 ALP Activity

The cells on TCP and patterned and unpatterned films with and without adsorbed ELP were cultured for 1, 2 and 3 weeks under static and dynamic conditions to study the effect of pattern, surface chemistry and mechanical stress on the phenotype expression during osteogenic differentiation.

During the active proliferation period, proteins related with cell cycle (e.g. histones) and cell growth (e.g. c-myc, c-fos, c-jun) are transcribed as well as proteins that form the ECM (type I collagen, fibronectin). Subsequently proliferation is down regulated and proteins associated with the bone cell phenotype are detected [128]. Alkaline phosphatase (ALP) is an early marker of the osteoblast differentiation [129]. It is an extracellular enzyme capable of splitting organic phosphate and thus it helps supply free phosphate necessary for the nucleation of hydroxyapatite crystals during the mineralization stage. ALP mRNA and enzyme activity can increase more than 10 fold in the cells [128].

ALP activity was determined on the 7th, 14th and 21st days of culture. ALP activity of cell lysates obtained from each sample was determined by spectrophotometric detection of the product of ALP activity at 405 nm every min for a total of twelve min at 25°C. The results were expressed as nmoles of substrate converted to product/min/sample, and nmoles of substrate converted to product/min/cell, which was named as specific ALP activity.

Generally, in the first week with the static group, the ALP activities were found to be low and they reached a maximum for all the samples at day 14 (*Fig.* 11) before decreasing again on Day 21. On Day 7 the highest ALP activity was obtained from St TCP followed by Dy TCP and this difference was probably due to the difference in the number of cells in the two wells (cell number on Dy TCP: 61.2×10^3, St TCP: 134.9×10^3).

The highest increase in ALP activity between Day 7 and Day 14 was observed with St P in the static group (87.2 fold) approaching the values on St P-ELP,

St UP-ELP and St UP. This steep increase of ALP activity on St P in the second week was probably due to rapid cell number increase (*Fig.* 9).

Day 7 ALP results obtained from dynamic group were generally lower than the static group, except St P. On day 14, the ALP activity on the films increased but decreased on the TCP of the dynamic group. Again the decrease of ALP activity on TCP can be ascribed to cell number decrease on Dy TCP in the second week and also to the low specific ALP activity of cells as seen on Figure 12. On day 21, the ALP activity on Dy P-ELP was significantly lower than the ALP activity on day 14 but for Dy UP-ELP and Dy UP, the differences in ALP activity between days 14 and 21 were not significant. The only exception among all the groups was Dy P, which had a significantly higher ALP activity on day 21 than day 14.
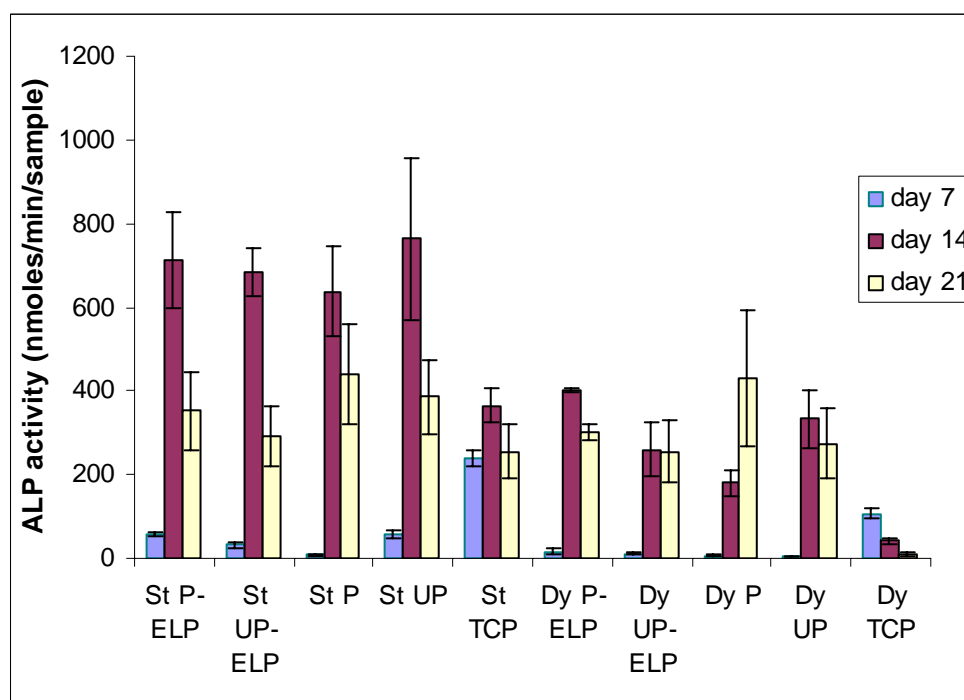
Figure 10. ALP activity on the polymeric films with different topography and surface chemistry cultured under static and dynamic conditions, and on TCP.

The specific ALP activities of Day 7 results were still lower than those of Day 14 results in static and dynamic groups with the only exception of Dy TCP, which followed a decreasing ALP activity trend of being the highest on Day 7 and the lowest on Day 21. However, when St TCP and Dy TCP were compared to each other, the specific ALP activity results at all time points were close to each other and the differences were not significant except on day 14.
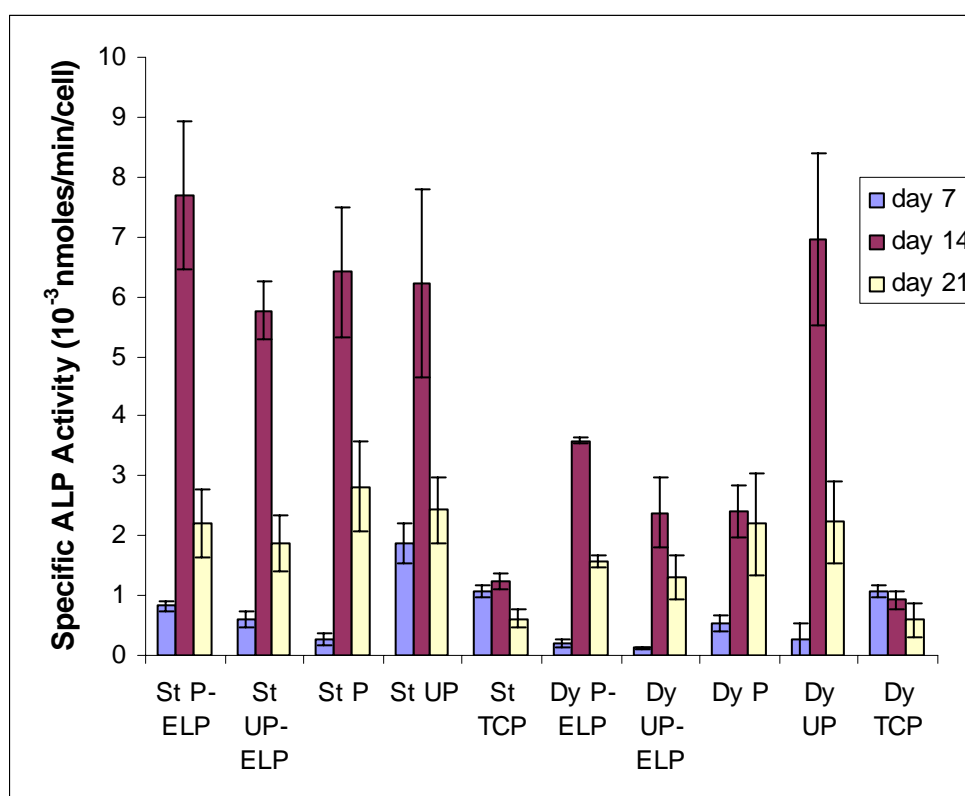
Figure 11. Specific ALP activity on the polymeric films with different topography and surface chemistry under static and dynamic conditions, and on TCP.

The dynamic culturing of cells was stopped at the end of Day 6 and cell culture was continued under static conditions. Specific ALP activities obtained for St P-ELP, St UP-ELP and St UP were much higher than their counterparts in the dynamic group on Day 7 (St P-ELP/Dy P-ELP: 4, St UP-ELP/Dy UP-ELP:

4.7, St UP/Dy UP: 7.2). There were two factors which could explain relatively low values of specific ALP activities obtained with the dynamic group; 1) decrease of temperature for short periods (29°C, 15 min) and, 2) tensile stress applied to the cells by the pNIPAM films during the temperature cycle. On the other hand the control groups (Dy TCP) did not receive any mechanical stress from the system and they were just exposed to cyclic temperature decreases. The similarity of specific ALP activities on St TCP, which were incubated at 37°C throughout the test, and Dy TCP suggests that temperature decrease has no noticable effect on the ALP activities of cells. In the literature, no information could be found about the relationship between temperature decrease and ALP activity change but in a study carried out by Lee et al., it was found that when pulp cells that were obtained from rat incisors cultured at 42°C for 30 min, ALP activity and expression increased significantly on day 7 and 14 compared with the control group that was maintained at 37°C [130]. Therefore it can be stated that the relative decrease in specific ALP activity observed in the dynamic group when compared to the static group was because of the tensile stress generated by the pNIPAM films under the defined conditions (cyclic temperature changes). Similar results have been reported by other groups working on effect of mechanical stress on osteoblast differentiation. Chen et al. applied strain mechanically to the level of 3% or 10% by surface elongation at 1 Hz for 8 or 48 h on human mesenchymal stem cells [131]. They also added another experimental group which included cells that rested for 48 h after cessation of mechanical stretching for 48 h to explore if the effects of mechanical stretching were transient. They found that 3% stretching induced upregulation of ALP gene expression at 8 h significantly but downregulation at 48 h and the value returned to the basal level of the unstretched control after the stretched cells had rested for 48 h. In the 10% stretched groups, the ALP mRNA level did not change significantly at 8 or 48 h but downregulated when the cells were left to relax for 48 h. Koike et al. used the bone marrow stromal cell line ST2 to investigate osteoblastic differentiation under 0.8%, 5%, 10%, and 15% elongation at 1 Hz for 2 days in a medium supplemented with 0.2mM ascorbic acid 2-phosphate and 5mM β-glycerophosphate [132]. They found that ALP activities of cells stretched by 0.8% and 5% significantly increased at 24h but no significant change in ALP activity was observed in the

5% elongation group at 48h. On the contrary, ALP activities of the 10% and 15% elongation groups significantly decreased.

In section 3.1.3, the deformation of cells was found to be above the physiologic conditions (2.2-10%) in this study, it was therefore concluded that the system applied high magnitude mechanical stress to the cells. It seems that magnitude of the mechanical stress may result in different response of cells in terms of ALP activity; high magnitude seems to lower the ALP activity, whereas low magnitude increases it.

In the second week, when cells were no longer cultured under dynamic conditions, increases in specific ALP activities were observed for all groups, except Dy TCP. The increases in specific ALP activities during the second week for the Dy P-ELP, Dy UP-ELP and Dy UP were much higher than their counterparts in the static group (St P-ELP, St UP-ELP and St UP), but still could not reach values comparable with theirs, except Dy-UP. This interesting finding might suggest that the ability of pNIPAM films to deliver mechanical stress differs when they are patterned and unpatterned, but it is not enough to explain the low specific ALP activity on Dy UP-ELP. It has been shown that ELP played a role in cell attachment leading to better cell-material interaction and retained the cells in attached form on the surface under dynamic conditions. Therefore, it can be stated that ELP adsorption enhanced the cell-material communication and thus cells received more mechanical stress. On the other hand, when there was no ELP on the surface, the cell-material interaction was not as good because of the formation of a hydration layer between the cells and pNIPAM when the temperature was decreased, but despite this disadvantage, patterns on the surface of pNIPAM (2 μm wide ridges and 10 μm wide grooves, a depth of 20 μm) might have increased the cell-material interaction by retaining the cells in the grooves.

On Day 21, the specific ALP activity results obtained from samples in the dynamic group decreased significantly when compared to Day 14 results, except Dy P. They were also comparable to the results obtained from their counterparts in the static group on the 21st day.

On Day 14 and 21, the specific ALP activity results obtained from all the pNIPAM films, both static and dynamic groups, were higher than those obtained from TCP suggest that pNIPAM films used in this study support the differentiation of BMSCs more than TCP. Smith et al. found that multipotent C2C12 cells exhibited ALP activity on RGD grafted p(NIPAM/NASI) surfaces significantly higher than those on TCP [17]. They did not observe a specific effect of RGD grafting on ALP activity of cells, and concluded that p(NIPAM/NASI) surfaces were more conductive for the expression of ALP.

3.3.3 Microscopic Examination

3.3.3.1 SEM

Scanning electron micrographs of cells cultured under static and dynamic conditions on patterned and unpatterned pNIPAM films were obtained at the end of 2 and 3 week incubation.

At the end of the second week, sheet-like cell layers were observed on the patterned films (*Fig.* 13). The cells were found to be attached on the side-walls of the grooves or within the grooves but stretched between the walls perpendicular to the axis. No difference was observed in cell attachment and density between ELP-adsorbed (*Fig.* 13 a, c) and ELP-free films (*Fig.* 13 b, d).

Day 21 micrographs of samples were similar to those of Day 14 in terms of cell attachment (*Fig.* 14). Cells were found within the grooves (*Fig.* 14 a, c, e, f) and stretched between the ridges (*Fig.* 14 b, d).
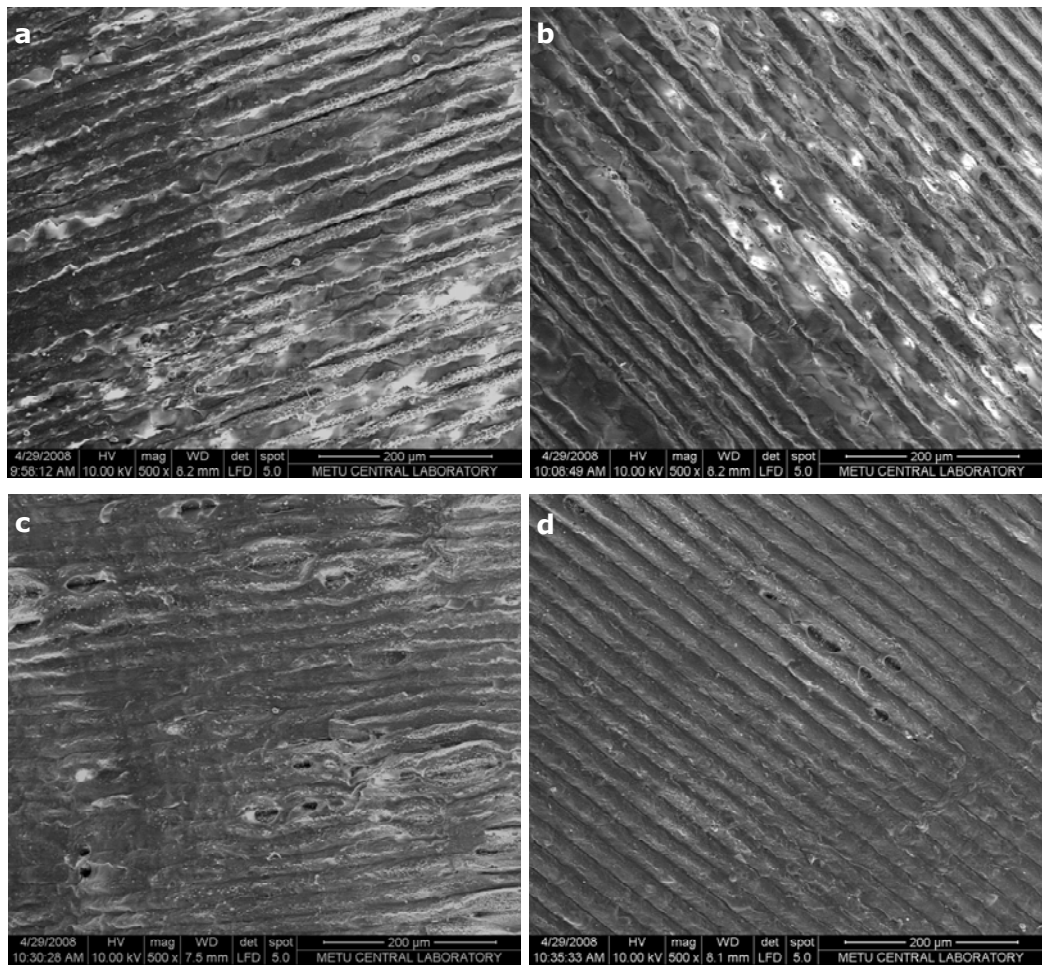
Figure 12. SEM micrographs of samples on Day 14 of culture. (a) Day 14 St P-ELP, (b) Day 14 St P, (c) Day 14 Dy P-ELP, (d) Day 14 Dy P. Magnification: x500
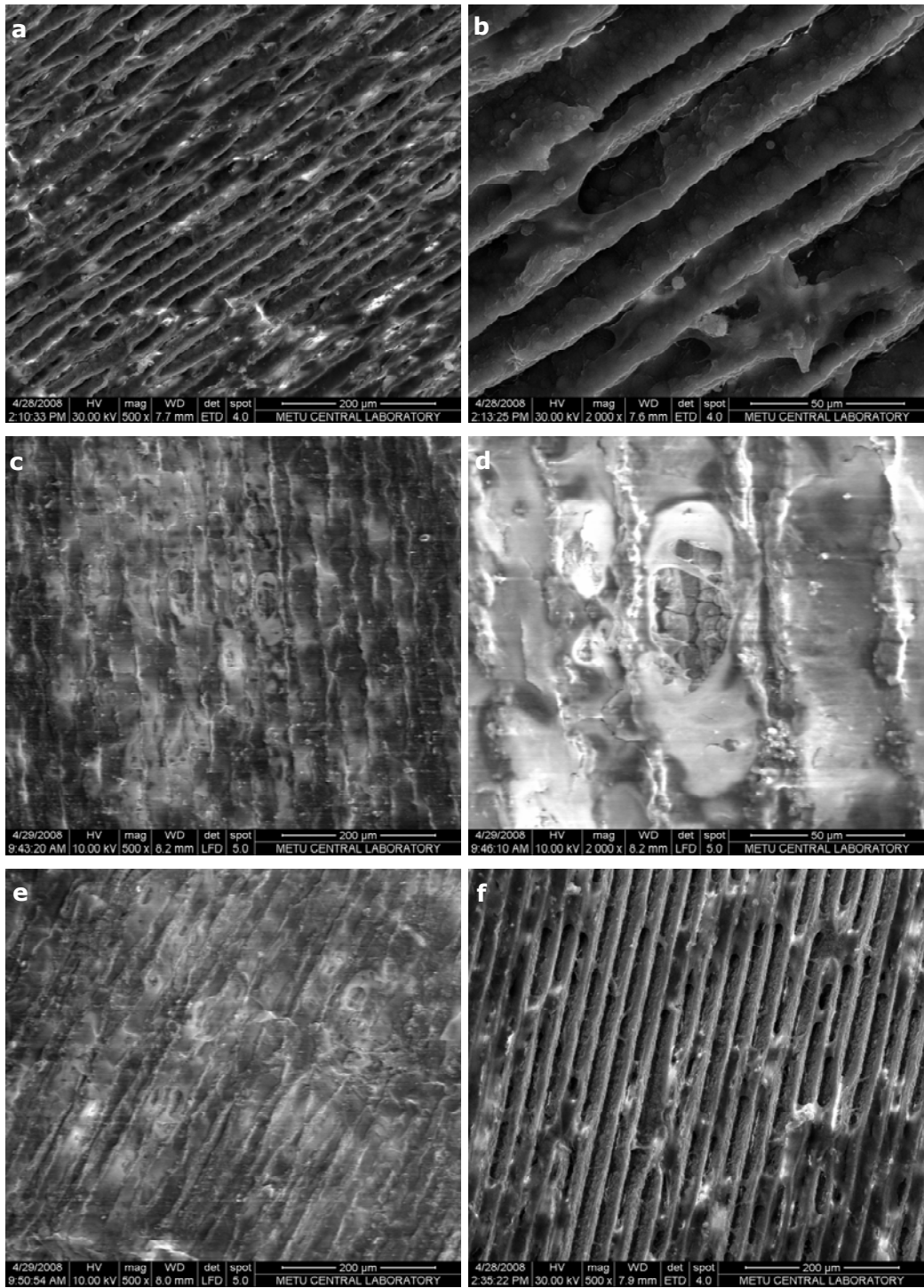
Figure 13. SEM micrographs of samples on Day 21 of culture. (a) Day 21 St P-ELP, x500 (b) Day 21 St P-ELP, x2000 (c) Day 21 St P, x500 (d) Day 21 St P, x2000 (e) Day 21 Dy P-ELP, x500 (f) Day 21 Dy P, x500

3.3.4 Mineralization

To detect mineralization on the films (to stain calcium phosphate) tetracycline (10 µg/mL) was introduced to the differentiation medium containing instead of penicillin (100 units/mL) and streptomycin (100 µg/mL) beginning from the 3rd day of culture. The pNIPAM films were fixed with 96% ethanol for 6 h. This step was carried out in a carbon dioxide incubator at 37°C to prevent the swelling of films, but this did not prevent them swelling in ethanol and they were swollen even at 37°C. The samples were examined with fluorescence microscopy at 480 nm (*Fig.* 15). Most of the samples had cracked due to swelling. Mineralization was observed over all the films. This finding, along with the ALP activity results (ALP activity of cells was higher on pNIPAM films than of those on TCP) suggests that pNIPAM can be considered as a good scaffold for enhanced osteogenic differentiation.
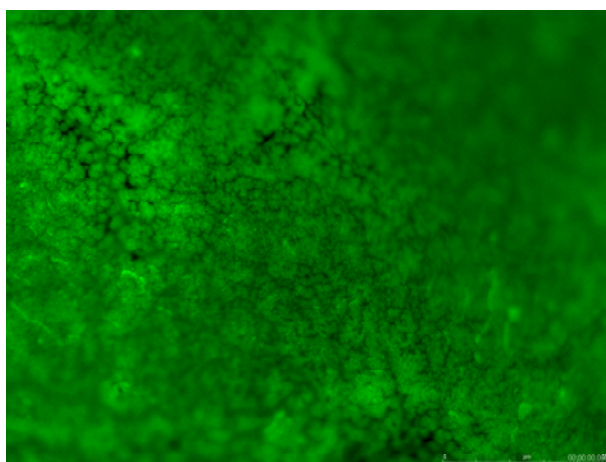
Figure 14. Fluorescense microscopy image of sample Dy UP-ELP on Day 21, Magnification: x10

XPS applied with scanning with scanning electron microscopy showed that calcium and phosphate were present on all of the cell-seeded samples which were fixed on Day 21. The ratio of calcium to phosphate was found to be 1.56 ± 0.21, which is close to the calcium/phosphate ratio of bone HAP (1.67).

CHAPTER 4

CONCLUSION

Stimuli-responsive (smart) polymers have a wide variety of applications in many areas of biotechnology. In this study, EGDMA crosslinked pNIPAM films were prepared by radical polymerization with UV in the presence of photoinitiator AIBN in the solvent isopropanol/water (1:1) with the ultimate goal of serving as intelligent cell carriers which can respond to temperature changes by altering their dimensions and apply mechanical stress on cells seeded onto them to achieve better healing. Thus, using the thermoresponsiveness of the polymer enabled the culturing of cells under dynamic conditions to study the effect of mechanical stress on the proliferation and differentiation of BMSCs into osteoblasts.

Patterns were formed on the surface of the polymers by using silicon wafers with microridges and grooves (groove width: 2 micrometer, ridge width: 10 micrometer, depth: 20 micrometer, wall angle: 54.7°) that were prepared by photolithography and wet etching techniques. The film surfaces were chemically modified by ELP-RGDx6 adsorption to promote cell adhesion with RGD amino acid sequences.

Swelling studies showed that the pNIPAM films had a LCST in the same range as those found in literature (~32°C). Dynamic culturing temperatures were chosen as 29 and 37°C, which are below and above the LCST, respectively, to induce hydrophilic/hydrophobic changes in the polymer resulting in dimension changes. The mechanical strain measured was found to vary between 2.2 and 10%, which is significantly more than the range observed with physiologically loaded bone.

ELP-RGD6 adsorbed surfaces had more cell numbers on the first day of culture, when all the cells were under static conditions, which shows that the

ELP-RGD6 adsorption enhanced cell attachment. The importance of the cell attachment sequences in ELP-RGD6 became more apparent when the cells were cultured under dynamic conditions. It was found that hydrophilic property of the polymer at 29°C resulted in decrease of cell number; comparable cell numbers were found on ELP adsorbed films in the dynamic group (Dy P-ELP, Dy UP-ELP) and the static group (St P-ELP, St UP-ELP). However, when the cyclic loadings were stopped, ELP-free films of the dynamic group reached comparable cell numbers with all the films in the static group. This finding showed that ELP adsorption enhanced initial cell attachment, but had no effect in cell proliferation in long term culturing. For the dynamic culture of the cells where temperature decrease was used, ELP was more crucial to retain cells on the films in attached form. A significantly high cell number decrease was observed on TCP in which cells were subjected to temperature changes but could not receive mechanical stress. On the other hand, the cells grown in dynamic culture showed an increase in number similar to the static group. This finding suggested that increased proliferation was a result of mechanical stress.

Specific ALP activity was used as a differentiation marker. They were highest on Day 14. Mechanical strain introduced to the cells in the dynamic group was found to decrease the specific ALP activity when compared with the cells in the static group. The only exception was Dy UP, which showed comparable specific ALP activity to those in static group. This finding suggested that the ability of pNIPAM films to transfer the mechanical stress on the cells differs when they are patterned and unpatterned. ELP adsorption was also thought to play an important role in transfer of mechanical stress by enhancing the cell-material interaction based on the decreased specific ALP activity on Dy UP-ELP films similar to Dy P-ELP films. The specific ALP results obtained from all the pNIPAM films, both static and dynamic, were higher than those obtained from TCP on Day 14 and 21. Therefore, it can be stated that pNIPAM films used in this study suppports the differentiation of BMSCs more than TCP.

To conclude, pNIPAM films were shown to be promising cell carriers to study the effect of mechanical stress on cells which can compete with the mechanical devices designed to load mechanical stress. ELP have proven

themselves as cell adhesion promoters, a property critical for tissue engineering.

REFERENCES

1. Grikscheit T. C., Vacanti J. P., *'The history and current status of tissue engineering: the future of pediatric surgery',* J Pediatr Surg*, 37 (3), 277-288 (2002).

2. McIntire L. V., Greisler H. P., Griffith L., Johnson P. C., Mooney D. J., Mrksich M., Parenteau N. L., Smith D., WTEC Panel Report on Tissue Engineering Research (2002).

3. Rotter N., Haisch A., Bücheler M., *'Cartilage and bone tissue engineering for reconstructive head and neck surgery'*, Eur Arch Otorhinolaryngol, 262 (7), 539–545 (2005).

4. Laurencin C. T., Ambrosio A. M. A., Borden M. D., Cooper J. A. Jr., *'Tissue engineering: orthopedic applications'*, Annu Rev Biomed Eng, 1, 19–46 (1999).

5. Burg K. J. L., Porter S., Kellam J. F., *'Biomaterial developments for bone tissue engineering',* Biomaterials, 22 (19), 2581-2593 (2001).

6. Rose F. R. A. J., Oreffo R. O. C., *'Bone tissue engineering: hope vs hype'* Biochem Biophys Res Commun, 292 (1), 1–7 (2002).

7. Ndreu A., Nikkola L., Ylikauppila H., Ashammakhi N., Hasirci V., *'Electrospun biodegradable nanofibrous mats for tissue engineering'*, Nanomedicine 3 (1), 45-60 (2008).

8. Hutmacher D. W., *'Scaffolds in tissue engineering bone and cartilage'*, Biomaterials 21 (24), 2529-2543 (2000).

9. Kenar H., Köse G. T., Hasirci V., *'Tissue engineering of bone on micropatterned biodegradable polyester films',* Biomaterials 27 (6), 885-895 (2006).

10. Vrana E., Builles N., Hindie M., Damour O., Aydinli A., Hasirci V., *'Contact guidance enhances the quality of a tissue engineered corneal stroma'* J Biomed Mater Res A, 84 (2), 454-463 (2008).

11. Zorlutuna P., Tezcaner A., Hasirci V., *'A novel construct as a cell carrier for tissue engineering',* J Biomater Sci Polym Ed, 19 (3), 399-410 (2008).

12. Jones J., Hench L. L., *'Regeneration of trabecular bone using porous ceramics',* Curr Opin Solid State Mater Sci, 7 (4-5), 301–307 (2003).

13. Gauthier O., Bouler J. M., Aguado E., Pilet P., Daculsi G., *'Macroporous biphasic calcium phosphate ceramics: influence of macropore diameter and macroporosity percentage on bone ingrowth',* Biomaterials, 11 (3), 133–139 (1998).

14. Karageorgiou V., Kaplan D., *'Porosity of 3D biomaterial scaffolds and osteogenesis',* Biomaterials, 26 (27), 5474-5491 (2005).

15. Mastrogiacomo M., Scaglione S., Martinetti R., Dolcini L., Beltrame F., Cancedda R., Quarto R., *'Role of scaffold internal structure on in vivo bone formation in macroporous calcium phosphate bioceramics',* Biomaterials, 27 (17), 3230–3237 (2006).

16. Mitchell S. A., Poulsson A. H. C., Davidson M. R., Emmison N., Shard A. G., Bradley R. H., *'Cellular attachment and spatial control of cells using micro-patterned ultra-violet/ozone treatment in serum enriched media',* Biomaterials, 25 (18), 4079-4086 (2004).

17. Smith E., Yang J., McGann L., Sebald W., Uludag H., *'RGD-grafted thermoreversible polymers to facilitate attachment of BMP-2 responsive C2C12 cells',* Biomaterials, 26 (35), 7329–7338 (2005).

18. So K., Fujibayashi S., Neo M., Anan Y., Ogawa T., Kokubo T., Nakamura T., 'A*ccelerated degradation and improved bone-bonding ability of hydroxyapatite ceramics by the addition of glass*', Biomaterials, 27 (27), 4738-4744 (2006).

19. Li X., Feng Q., Cui F., '*In vitro degradation of porous nano-hydroxyapatite/collagen/PLLA scaffold reinforced by chitin fibres*', Mater Sci and Eng: C, 26 (4), 716-720 (2006).

20. Luo Z. S., Cui F. Z., Feng Q. L., Li H. D., Zhu X. D., Spector M., '*In vitro and in vivo evaluation of degradability of hydroxyapatite coatings synthesized by ion beam-assisted deposition*', Surf Coat Technol, 131 (1-3), 192-195 (2000).

21. Hasirci V., Lewandrowski K., Gresser J. D., Wise V., Trantolo D. J., '*Versatility of biodegradable biopolymers: degradability and an in vivo application*', J Biotechnol, 86 (2), 135-150 (2001).

22. Spector M., '*Biomaterials-based tissue engineering and regenerative medicine solutions to musculoskeletal problems*', Swiss Med Wkly, 136, 293–301 (2006).

23. Cheung H. Y., Lau K. T., Lu T. P., Hui D., '*A critical review on polymer-based bio-engineered materials for scaffold development*,' Composites Part B: Eng, 38 (3), 291-300 (2007).

24. Meinel L., Hofmann S., Karageorgiou V., Zichnew L., Langer R., Kaplan D., Vunjak-Novakovic G., '*Engineering cartilage-like tissue using human mesenchymal stem cells and silk protein scaffolds*', Biotechnol Bioeng, 88, 379-391 (2004).

25. Meyer U., Büchter A., Wiesmann H. P., Joos U., Jones D. B., '*Basic reactions of osteoblasts on structured material surfaces*', Eur Cell Mater, 9, 39-49 (2005).

26. Ashammakhi N., Ndreu A., Piras A. M., Nikkola L., Sindelar T., Ylikauppila H., Harlin A., Gomes M. E., Neves N. M., Chiellini E., Chiellini F., Hasirci V., Redl H., Reis R. L. *'Biodegradable nanomats produced by electrospinning: expanding multifunctionality and potential for tissue engineering'*, J Nanosci Nanotechnol, 7 (3), 862-882 (2007).

27. Liu X., Ma P. X., *'Polymeric scaffolds for bone tissue engineering'*, Ann Biomed Eng, 32 (3), 477–486 (2004).

28. Lee S. H., Shin H., *'Matrices and scaffolds for delivery of bioactive molecules in bone and cartilage tissue engineering'*, Advan Drug Del Rev, 59 (4-5), 339-359 (2007).

29. Habraken W. J. E. M., Wolke J. G. C., Jansen J. A., *'Ceramic composites as matrices and scaffolds for drug delivery in tissue engineering'*, Advan Drug Del Rev, 59 (4-5), 234–248 (2007).

30. Hutmacher D. W., Schantz J. T., Lam C. X., Tan K. C., Lim T. C., *'State of the art and future directions of scaffold-based bone engineering from a biomaterials perspective'*, J Tissue Eng Regen Med, 1 (4), 245–260 (2007).

31. Mano J. F., Silva G. A., Azevedo H. S., Malafaya P. B., Sousa R. A., Silva S. S., Boesel L. F., Oliveira J. M., Santos T. C., Marques A. P., Neves N. M., Reis R. L., *'Natural origin biodegradable systems in tissue engineering and regenerative medicine: present status and some moving trends'*, J R Soc Interface, 4 (17), 999–1030 (2007).

32. Rodríguez-Cabello J. C., Reguera J., Girotti A., Alonso M., Testera A. M., *'Developing functionality in elastin-like polymers by increasing their molecular complexity: the power of the genetic engineering approach'*, Prog Polym Sci 30 (11), 1119–1145, (2005).

33. Tirrell D. A., *'Mechanical properties of artificial protein matrices engineered for control of cell and tissue behavior'*, Macromolecules, 36 (5), 1553–1558 (2003).

34. Girotti A., Reguera J., Rodríguez-Cabello J. C., Arias F. J., Alonso M., Testera A. M., *'Design and bioproduction of a recombinant multi(bio)functional elastin-like protein polymer containing cell adhesion sequences for tissue engineering purposes'*, J Mater Sci Mater Med, 15 (4), 479–484 (2004).

35. Urry D. W., 'Molecular machines: how motion and other functions of living organism can result from reversible chemical changes', Angew Chem Int Edit Eng, 32 (6), 819–841 (1993).

36. Seal B. R., Otero T. C., Panitch A., '*Polymeric biomaterials for tissue and organ regeneration'*, Mater Sci Eng, 34 (4-5), 147-230 (2001).

37. Cancedda R., Dozin B., Giannoni P., R. Quarto, '*Tissue engineering and cell therapy of cartilage and bone',* Matrix Biol, 22 (1), 81-91 (2003).

38. Kim J., Kim I. S., Cho T. H., Lee K. B., Hwang S. J., Tae G., Noh I., Lee S. H., Park Y., Sun K., '*Bone regeneration using hyaluronic acid-based hydrogel with bone morphogenic protein-2 and human mesenchymal stem cells',* Biomaterials, 28 (10), 1830-1837 (2007).

39. Grigolo B., Roseti L., Fiorini M., Fini M., Giavaresi G., Aldini N. N., Giardino R., Facchini A., '*Transplantation of chondrocytes seeded on a hyaluronan derivative (hyaff-11) into cartilage defects in rabbits'*, Biomaterials 22 (17), 2417–2424 (2001).

40. Martinoa A. D., Sittingerc M., Risbud M. V., *'Chitosan: A versatile biopolymer for orthopaedic tissue-engineering',* Biomaterials, 26 (30), 5983-5990 (2005).

41. Chen G. Q., Wu Q., *'The application of polyhydroxyalkanoates as tissue engineering materials'*, Biomaterials, 26, 6565–78 (2005).

42. Köse G. T., Kenar H., Hasirci N., Hasirci V., *'Macroporous poly(3-hydroxybutyrate-co-3-hydroxyvalerate) matrices for bone tissue engineering'*, Biomaterials, 24 (11), 1949-1958 (2003).

43. Köse G. T., Korkusuz F., Korkusuz P., Purali N., Ozkul A., Hasirci V., *'Bone generation on PHBV matrices: an in vitro study'*, Biomaterials, 24 (27), 4999-5007 (2003).

44. Altman G. H., Diaz F., Jakuba C., Calabro T., Horan R. L., Chen J. S., Lu H., Richmond J, Kaplan D. L., *'Silk-based biomaterials'*, Biomaterials, 24 (3), 401–416 (2003).

45. Rezwan K., Chen Q. Z., Blaker J. J., Boccaccini A. R., *'Biodegradable and bioactive porous polymer/inorganic composite scaffolds for bone tissue engineering',* Biomaterials, 27 (18), 3413–3431 (2006).

46. Dunn A. S., Campbell P. G., Marra K. G., *'The influence of polymer blend composition on the degradation of polymer/hydroxyapatite biomaterials'*, J Mater Sci Mater Med, 12 (8), 673–677 (2001).

47. Rich J., Jaakkola T., Tirri T., Narhi T., Y-Urpo A., Seppala J., *'In Vitro evaluation of poly(ε-caprolactone-co-DL-lactide)/bioactive glass composites'*, Biomaterials, 23 (10), 43–2150 (2002).

48. Yang S., Leong K. F., Du Z., Chua C. K., *'The design of scaffolds for use in tissue engineering. Part I. Traditional factors',* Tissue Eng, 7 (6), 679–689 (2001).

49. Stallmann H. P., Faber C., Bronckers A. L. J. J., Nieuw Amerongen A. V., Wuisman P. I. J. M., *'In vitro gentamycin release from commercially available calcium–phosphate bone substitutes influence of carrier type on duration of the release profile'*, BMC Musculoskelet Disord, 7 (18), 1–8 (2006).

50. Yuan H., Van Den Doel M., Li S., Van Blitterswijk C. A., De Groot K., De Bruijn J. D., *'A comparison of the osteoinductive potential of two calcium phosphate ceramics implanted intramuscularly in goats'*, J Mater Sci Mater Med, 13 (12), 1271–1275 (2002).

51. Xu H. H. K., Weir M. D., Burguera E. F., Fraser A. M., *'Injectable and macroporous calcium phosphate cement scaffold'*, Biomaterials, 27 (24), 4279-4287 (2006).

52. Le Nihouannen D., Saffarzadeh A., Aguado E., Goyenvalle E., Gauthier O., Moreau F., Pilet P., Spaethe R., Daculsi G., Layrolle P., *'Osteogenic properties of calcium phosphate ceramics and fibrin glue based composites'*, J Mater Sci Mater Med, 18 (2), 225–235 (2007).

53. Vallet-Regí M., González-Calbet J. M., *'Calcium phosphates as substitution of bone tissues'*, Prog Solid State Chem, 32 (1-2), 1–31 (2004).

54. Meseguer-Olmo L., Ros-Nicolás M. J., Clavel-Sainz M., Vicente-Ortega V., Alcaraz-Baños M., Lax-Pérez A., Arcos D., Ragel C. V., Vallet-Regí M., *'Biocompatibility and in vivo gentamicin release from bioactive sol-gel glass implants'*, J Biomed Mater Res, 61 (3), 458-465 (2002).

55. Ratier A., Gibson I. R., Best S. M., Freche M., Lacout J. L., Rodriguez F., *'Setting Characteristics and Mechanical Behaviour of a Calcium Phosphate Bone Cement Containing Tetracycline'*, Biomaterials, 22 (9), 897-901 (2001).

56. Yan X. X., Deng H. X., Huang X. H., Lu G. Q., Qiao S. Z., Zhao D. Y., Yu C.Z., *'Mesoporous bioactive glasses. I. Synthesis and structural characterization'*, J Non-Cryst Solids, 351 (40-42), 3209–3217 (2005).

57. Vallet-Regí M., Arcos D., *'Silicon substituted hydroxyapatites. A method to upgrade calcium phosphate based implants'*, J Mater Chem, 15 (15), 1509–1516 (2005).

58. Kim H. M., *'Ceramic bioactivity and related biomimetic strategy'*, Curr Opin in Solid State Mater Sci, 7 (4-5), 289-299 (2003).

59. Holand W., Volker Rheinberger V., Apel E., Hoen C., Holand M., Dommann A., Obrecht M., Mauth C., Graf-Hausner U., *'Clinical applications of glass-ceramics in dentistry'*, J Mater Sci Mater Med, 17 (11), 1037–1042 (2006).

60. Kang S. W., Yang H. S., Seo S. W., Han D. K., Kim B. S., '*Apatite-coated poly(lactic-co-glycolic acid) microspheres as an injectable scaffold for bone tissue engineering*', J Biomed Mater Res A, 85 (3), 747-756 (2008).

61. Gil E. S., Hudson S. M., '*Stimuli-reponsive polymers and their bioconjugates*', Prog Polym Sci, 29 (12), 1173–1222 (2004)

62. Pinkrah V. T., Snowden M. J., Mitchell J. C., Seidel J., Chowdhry B. Z., Fern G. R., '*Physicochemical properties of poly(N-isopropylacrylamide-co-4-vinylpyridine) cationic polyelectrolyte colloidal microgels*', Langmuir, 19 (3), 585–90 (2003)

63. Peng T., Cheng Y. L., '*PNIPAAm and PMAA co-grafted porous PE membranes: living radical co-grafting mechanism and multi-stimuli responsive permeability*', Polymer, 42 (5), 2091–2100 (2001).

64. Bignotti F., Penco M., Sartore L., Peroni I., Mendichi R., Casolaro M., D'Amore A., '*Synthesis, characterisation and solution behaviour of thermo-and pH-responsive polymers bearing L-leucine residues in the side chains*', Polymer, 41 (23), 8247–8256 (2000)

65. Gan L. H., Gan Y. Y., Deen G. R., '*Poly(N-acryloyl-N'-propylpiperazine): a new stimuli-responsive polymer*', Macromolecules, 33 (21), 7893–7897 (2000)

66. Kurisawa M., Yui N., '*Dual-stimuli-responsive drug release from interpenetrating polymer network-structured hydrogels of gelatin and dextran*', J Control Release, 54 (2), 191–200 (1998).
67. Jeong B., Gutowska A., '*Lessons from nature: stimuliresponsive polymers and their biomedical applications*', Trends Biotechnol, 20 (7), 305–311 (2002)

68. Anastase-Ravion S., Ding Z., Pelle A., Hoffman A.S., Letourneur D., '*New antibody purification procedure using a thermally responsive poly(N-isopropylacrylamide)-dextran derivative conjugate*', J Chromatogr B, 761 (2), 247–254 (2001)

69. Meyer D. E., Chilkoti A., *'Purification of recombinant proteins by fusion with thermally-responsive polypeptides'*, Nat Biotechnol 17 (11), 1112–1115 (1999)

70. Meyer D. E., Trabbic-Carlson K., Chilkoti A., *'Protein purification by fusion with an environmentally responsive elastinlike polypeptide: effect of polypeptide length on the purification of thioredoxin'*, Biotechnol Prog, 17 (4), 720–728 (2001).

71. Irvin D. J., Goods S. H., Whinnery L. L., *'Direct measurement of extension and force in a conductive polymer gel actuator'*, Chem Mater, 13 (4), 1143–1145 (2001).

72. Huber D. L., Manginell R. P., Samara M. A., Kim B., Bunker B. C., *'Programmed adsorption and release of proteins in a microfluidic device'* Science, 301 (5631), 352–354 (2003).

73. Beebe D. J., Moore J. S., Bauer J. M., Yu Q., Liu R. H., Devadoss C., Jo B. H., *'Functional hydrogel structures for autonomous flow control inside microfluidic channels'*, Nature, 404 (6778), 588–590 (2000).

74. Yokoyama M., *'Gene delivery using temperature-responsive polymeric carriers'*, Drug Discov Today, 7 (7), 426–432 (2002).

75. Kurisawa M., Yokoyama M., Okano T., *'Gene expression control by temperature with thermo-responsive polymeric gene carriers'*, J Control Release, 69 (1), 127–137 (2000).

76. Meyer D. E., Shin B. C., Kong G. A., Dewhirst M. W., Chilkoti A., *'Drug targeting using thermally responsive polymers and local hyperthermia'*, J Control Release, 74 (1-3), 213–224 (2001).

77. Weidner J., 'Drug targeting using thermally responsive polymers and local hyperthermia' Drug Discov Today, 6 (23), 1239–1241 (2001).

78. Kim I. S., Jeong Y. I., Cho C. S., Kim S. H., *'Thermo-responsive selfassembled polymeric micelles for drug delivery in vitro'*, Int J Pharm, 205 (1-2),165–172 (2000).

79. Kakoulides E. P., Smart J. D., Tsibouklis J., 'Azocross-linked poly(acrylic acid) for colonic delivery and adhesion specificity: synthesis and characterization', J Control Release, 52 (3), 291–300 (1998).

80. Shantha K. L., Harding D. R. K., *'Preparation and in-vitro evaluation of poly[N-vinyl-2-pyrrolidone-polyethylene glycol diacrylate]-chitosan interpolymeric pH-responsive hydrogels for oral drug delivery'*, Int J Pharm, 207 (1-2), 65–70 (2000).

81. Meyer D. E., Kong G. A., Dewhirst M. W., Zalutsky M. R., Chilkoti A., *'Targeting a genetically engineered elastin-like polypeptide to solid tumors by local hyperthermia'*, Cancer Res, 61 (4), 1548–1554 (2001).

82. Okano T., Yamada N., Okuhara M., Sakai H., Sakurai Y., *'Mechanism of cell detachment from temperature-modulated, hydrophilic–hydrophobic polymer surfaces'*, Biomaterials, 16 (4), 297–303 (1995).

83. Nakajima K., Honda S., Nakamura Y., Lopéz-Redondo F., Kohsaka S., Yamato M., Kikuchi A., Okano T., *'Intact microglia are cultured and non-invasively harvested without pathological activation using a novel cultured cell recovery method'*, Biomaterials, 22 (11), 1213–1223 (2001).

84. Yamato M., Konno C., Kushida A., Hirose M., Utsumi M., Kikuchi A., Okano T., *'Release of adsorbed fibronectin from temperature-responsive culture surfaces requires cellular activity'*, Biomaterials, 21 (10), 981–986 (2000).

85. Nandkumar M. A., Yamato M., Kushida A., Konno C., Hirose M., Kikuchi A., Okano T., *'Two-dimensional cell sheet manipulation of heterotypically co-cultured lung cells utilizing temperature-responsive culture dishes results in long-term maintenance of differentiated epithelial cell functions'*, Biomaterials, 23 (4), 1121–1130 (2002).

86. Uchida K., Sakai K., Ito E., Kwon O. H., Kikuchi A., Yamato M., Okano T., *'Temperature-dependent modulation of blood platelet movement and morphology on poly(N-isopropylacrylamide)- grafted surfaces'*, Biomaterials, 21 (9), 923–929 (2000).

87. Ebara M., Yamato M., Hirose M., Aoyagi T., Kikuchi A., Sakai K., Okano T., *'Copolymerization of 2-carboxyisopropylacrylamide with N-isopropylacrylamide accelerates cell detachment from grafted surfaces by reducing temperature'*, Biomacromolecules, 4 (2), 344–349 (2003).

88. Kim M. R., Jeong J. H., Park T. G., *'Swelling Induced detachment of chondrocytes using RGD-modified poly(N-isopropylacrylamide) hydrogel beads'*, Biotechnol Prog, 18 (3), 495–500 (2002).

89. Shimizu T., Yamato M., Kikuchi A., Okano T., *'Cell sheet engineering for myocardial tissue reconstruction'*, Biomaterials, 24 (13), 2309-2316 (2003).

90. Yamada N., Okano T., Sakai H., Karikusa F., Sawasaki Y., Sakurai Y., *'Thermo-responsive polymeric surfaces; control of attachment and detachment of cultured cells'*, Macromol Rapid Commun, 11 (11), 571-576 (1990).

91. de las Heras Alarcon C., Pennadam S., Alexander C., *'Stimuli responsive polymers for biomedical applications'*, Chem Soc Rev, 34 (3), 276–285 (2005).

92. Yang J., Yamato M., Shimizu T., Sekine H., Ohashi K., Kanzaki M., Ohki T., Nishida K., Okano T., *'Reconstruction of functional tissues with cell sheet engineering'*, Biomaterials, 28 (34), 5033–5043 (2007).

93. Shimizu T., Sekine H., Yang J., Isoi Y., Yamato M., Kikuchi A., Kobayashi E., Okano T., *'Polysurgery of cell sheet grafts overcomes diffusion limits to produce thick, vascularized myocardial tissues'*, FASEB J, 20 (6), 708–710 (2006).

94. Sekine H., Shimizu T., Kosaka S., Kobayashi E., Okano T., *'Cardiomyocyte bridging between hearts and bioengineered myocardial tissues with mesenchymal transition of mesothelial cells'*, J Heart Lung Transplant, 25 (3), 324–332 (2006).

95. Sekine H., Shimizu T., Yang J., Kobayashi E., Okano T., *'Pulsatile myocardial tubes fabricated with cell sheet engineering'*, Circulation, 114 (1 Suppl.), I87–193 (2006).

96. Nishida K., Yamato M., Hayashida Y., Watanabe K., Yamamoto K., Adachi E., Nagai S., Kikuchi A., Maeda N., Watanabe H., Okano T., Tano Y., *'Corneal reconstruction with tissue-engineered cell sheets composed of autologous oral mucosal epithelium'*, N Engl J Med, 351 (12), 1187–1196 (2004).

97. Ohki T., Yamato M., Murakami D., Takagi R., Yang J., Namiki H., Okano T., Takasaki K., *'Treatment of oesophageal ulcerations using endoscopic transplantation of tissue-engineered autologous oral mucosal epithelial cell sheets in a canine model'*, Gut, 55 (12), 1704–1710 (2006).

98. Kanzaki M., Yamato M., Hatakeyama H., Kohno C., Yang J., Umemoto T., Kikuchi A., Okano T., Onuki T., *'Tissue engineered epithelial cell sheets for the creation of a bioartificial trachea'*, Tissue Eng, 12 (5), 1275–83 (2006).
99. Kikuchi A., Okano T., *'Regeneration of tissues and organs – new technique opens up new possibilities for regenerative medicine through control of interaction of polymers with water -'*, Nitto Denko Technical Report, 85 (42), 44-48 (2004).

100. Tsuda Y., Kikuchi A., Yamato M., Chen G., Okano T., *'Heterotypic cell interactions on a dually patterned surface'*, Biochem Biophys Res Commun, 348 (3), 937–944 (2006).

101. Drury J. L., Mooney D. J., *'Hydrogels for tissue engineering: scaffold design variables and applications'*, Biomaterials, 24 (24), 4337–4351 (2003).

71

102. Stile R. A., Healy K. E., *'Thermo-responsive peptide-modified hydrogels for tissue regeneration'*, Biomacromolecules, 2 (1), 185-194 (2001).

103. Kim S., Healy K. E., *'Synthesis and characterization of injectable poly(N-isopropylacrylamide-co-acrylic acid) hydrogels with proteolytically degradable cross-links'*, Biomacromolecules, 4 (5), 1214-1223 (2003).

104. Urry D. W., Luan C. H., Parker T. M., Gowda D. C., Prasad K. U., Reid M. C., Safavy A., *'Temperature of polypeptide inverse temperature transition depends on mean residue hydrophobicity'*, J Am Chem Soc, 113 (11), 4346-4348 (1991).

105. Betre H., Ong S. R., Guilak F., Chilkoti A., Fermor B., Setton L. A., *'Chondrocytic differentiation of human adipose-derived adult stem cells in elastin-like polypeptide'*, Biomaterials, 27 (1), 91-99 (2006).

106. McHale M. K., Setton L. A., Chilkoti A., *'Synthesis and in vitro evaluation of enzymatically cross-linked elastin-like polypeptide gels for cartilaginous tissue repair'*, Tissue Eng, 11 (11-12), 1768-1779 (2005).

107. Wang J. H. C., Thampatty B. P., *'An introductory review of cell mechanobiology'*, Biomech Model Mechanobiol, 5 (1), 1–16 (2006).

108. Vico L., Collet P., Guignandon A., Lafage-Proust M. H., Thomas T., Rehailia M., Alexandre C., *'Effects of long-term microgravity exposure on cancellous and cortical weight-bearing bones of cosmonauts'*, Lancet, 355 (9215), 1607-1611 (2000).

109. Leblanc A. D., Schneider V. S., Evans H. J., Engelbretson D. A., Krebs J. M., *'Bone mineral loss and recovery after 17 weeks of bed rest'*, J Bone Miner Res, 5 (8), 843-850 (1990).

110. Simkin A., Ayalon J., Leichter I., *'Increased trabecular bone density due to boneloading exercises in postmenopausal osteoporotic women'*, Calcif Tissue Int, 40, 59-63 (1987).

111. Knothe Tate M. L., Steck R., Forwood M. R., Niederer P., *'In vivo demonstration of load-induced fluid flow in the rat tibia and its potential implications for processes associated with functional adaptation'*, J Exp Biol, 203 (pt 18), 2737-2745 (2000).

112. Leclerc E., David B., Griscom L., Lepioufle B., Fujii T., Layrolle P., Legallaisa C., *'Study of osteoblastic cells in a microfluidic environment'*, Biomaterials, 27 (4), 586–595 (2006).

113. Meyer U., Büchter A., Nazer N., Wiesmann H. P., *'Design and performance of a bioreactor system for mechanically promoted three-dimensional tissue engineering'*, Br J Oral Maxillof Surg, 44 (2), 134–140 (2006).

114. Li J., Chen G., Zheng L., Luo S., Zhao Z., *'Osteoblast cytoskeletal modulation in response to compressive stress at physiological levels'*, Mol Cell Biochem, 304 (1-2), 45–52 (2007).

115. Walboomers X. F., Elder S. E., Bumgardner J. D., Jansen J. A., *'Hydrodynamic compression of young and adult rat osteoblast-like cells on titanium fiber mesh'*, J Biomed Mater Res A, 76 (1), 16-24 (2006)

116. Masuda T., Takahashi I., Anada T., Arai F., Fukuda T., Takano-Yamamoto T., Suzuki O., *'Development of a cell culture system loading cyclic mechanical strain to chondrogenic cells'*, J Biotechnol, 133 (2), 231–238 (2008).

117. Suzuki O., Takahashi I., Kamakura S., Sasaki K., Kamijo R., Nakamura M., Oda M., Uchida T., Arai F., Fukuda T., 'Effects of mechanical stress and scaffold material on osteogenesis and chondrogenesis', Micro-NanoMechatronics and Human Science, 2005 IEEE International Symposium, 235-240 (2005).

118. Takahashi I., Onodera K., Sasano Y., Mizoguchi I., Bae J. W., Mitani H., Kagayama M., Mitani H., *'Effect of stretching on gene expression of β1 integrin and focal adhesion kinase and on chondrogenesis through cell-extracellular matrix interactions'*, Eur J Cell Biol, 82 (4), 182-192 (2003).

119. Di Palma F., Douet M., Boachon C., Guignandon A., Peyroche S., Forest B., Alexandre C., Chamson A., Rattner A., *'Physiological strains induce differentiation in human osteoblasts cultured on orthopaedic biomaterial'*, Biomaterials, 24 (18), 3139–3151 (2003).

120. Yun J. K., Anderson J. M., Ziats N. P., *'Cyclic strain effects on human monocyte interactions with endothelial cells and extracellular matrix proteins'*, Tissue Eng, 5 (1), 67-77 (1999)

121. Kaspar D., Seidl W., Neidlinger-Wilke C., Beck A., Claes L., Ignatius A., *'Proliferation of human-derived osteoblast-like cells depends on the cycle number and frequency of uniaxial strain'*, J Biomech, 35 (7), 873–880 (2002).

122. Kim Y. S., Lim J. Y., Donahue H. J., Lowe T. L., *'Thermoresponsive terpolymeric films applicable for osteoblastic cell growth and noninvasive cell sheet harvesting'*, Tissue Eng, 11 (1/2), 30-40 (2005).

123. Brazel C. S., Peppas N. A., *'Synthesis and Characterization of Thermo- and Chemomechanically Responsive Poly(N-isopropylacrylamide-co-methacrylic acid) Hydrogels'*, Macromolecules, 28 (24), 8016-8020 (1995).
124. Matsuzaka K., Walboomers X. F., de Ruijter J. E., Jansen J. A., *'The effect of poly-L-lactic acid with parallel surface micro groove on osteoblast-like cells in vitro'*, Biomaterials, 20 (14), 1293-1301 (1999).

125. Ignatius A., Blessing H., Liedert A., Schmidt C., Neidlinger-Wilke C., Kaspar D., Friemert B., Claes L., *'Tissue engineering of bone: effects of mechanical strain on osteoblastic cells in type I collagen matrices'*, Biomaterials, 26 (3), 311–318 (2005).

126. Claes L. E., Heigele C. A., Neidlinger-Wilke C., Kaspar D., Seidl W., Margevicius K. J., Augat P., *'Effects of mechanical factors on the fracture healing process'*, Clin Orthop Relat Res, 355 (Suppl), 132–147 (1998).

127. Li-Bo Chen L. B., Xiao-Bing Jiang X. B., Lian Yang L., *'Differentiation of rat marrow mesenchymal stem cells into pancreatic islet beta-cells'*, World J Gastroenterol, 10 (20), 3016-3020 (2004).

128. Stein G. S., Lian J. B., *'Molecular Mechanisms mediating proliferation/differentiation interrelationships during progressive development of osteoblast phenotype'*, Endocr Rev, 14 (4), 424-441 (1993).

129. Ozawa S., Kasugai S., *'Evaluation of implant materials (hydroxyapatite, glass-ceramics, titanium) in rat bone marrow stromal cell culture'*, Biomaterials, 17 (1), 23–29 (1996).

130. Lee M. W., Muramatsu T., Uekusa T., Lee J. H., Shimono M., *'Heat stress induces alkaline phosphatase activity and heat shock protein 25 expression in cultured pulp cells'*, Int Endod J, 41 (2), 158–162 (2008).

131. Chen Y. J., Huang C. H., Lee I. C., Lee Y. T., Chen M. H., Young T. H., *'Effects of cyclic mechanical stretching on the mRNA expression of tendon/ligament-related and osteoblast-specific genes in human mesenchymal stem cells'*, Connect Tissue Res, 49 (1), 7–14 (2008).

132. Koike M., Shimokawa H., Kanno Z., Ohya K., Soma K., *'Effects of mechanical strain on proliferation and differentiation of bone marrow stromal cell line ST2'*, J Bone Miner Metab, 23 (3), 219–225 (2005).

APPENDIX A

CALIBRATION CURVE FOR PROLIFERATION

The graph shows Dye Reduction (%) on the y-axis (0 to 10) versus Cell Number ($\times 10^3$) on the x-axis (0 to 250).

$$y = 0{,}0423x$$
$$R^2 = 0{,}998$$
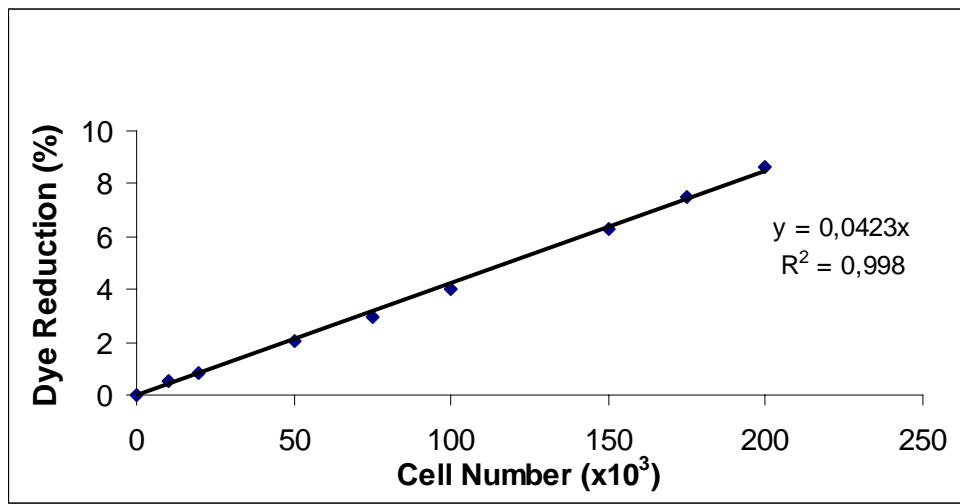
Figure 15. Calibration curve for BMSCs prepared by Alamar Blue assay.

APPENDIX B

ALP CALIBRATION CURVE
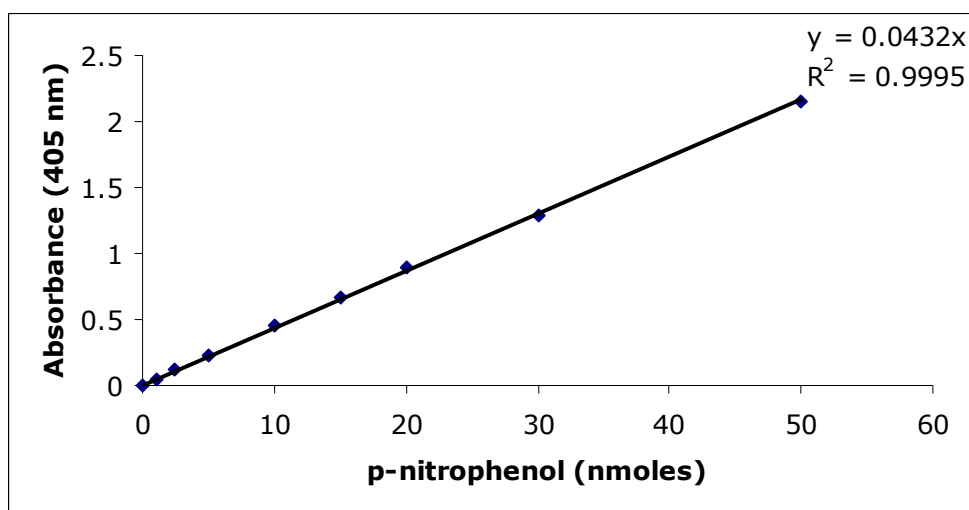
Figure 16. ALP calibration curve prepared with p-nitrophenol.